UNIVERSITY OF MICHIGAN
DEPARTMENT OF MECHANICAL ENGINEERING
CAVITATION AND MULTIPHASE FLOW LABORATORY

Report No. UMICH 013503-4-PR

PROGRESS REPORT NO. 4 - ARGONNE NATIONAL LABORATORY

Contract No. 31-109-Eng.-38

by

F. G. Hammitt
J-B. Hwang
M. K. De
A. N. El Hasrouni
S. A. Barber
G. N. Chammas

June, 1976

I. Introduction

As explained quite thoroughly in previous reports (1,eg), we are attempting to develop the capability for predicting eventual mechanical cavitation damage rates to be encountered in field devices (in particular sodium pumps) from essentially instantaneous measurements using the bubble collapse pulse spectrum as the operative signal. In principle, we wish to obtain the spectrum of cavitation bubble collapse pulse impulse, as applied to a microprobe, in the region where damage is expected. Ideally, the active element of the probe should be immersed in the sodium. However, for practical reasons in these experiments, which are essentially "first of a kind", it has been found necessary to use wave-guide probes (1) where the active element is at essentially room temperature, but remote from the sodium. The "wave-guide" of course induces some undesirable and unknown signal distortion and attenuation

It now appears possible in the present state-of-the art to develop a suitable direct submergence microprobe, and this should of course be done if follow-on work were contemplated. Also a method for direct calibration of probes between measured input impulse and output pulse-count spectrum should be developed. We are now doing this under a related ONR contract.

In spite of the relatively crude pulse measuring set-up employed in these initial experiments in a vibratory cavitation damage facility, meaningful ($\lessdot$25% standard error) correlations have been obtained between pulse-count integrated energy spectrum and measured damage rate (mean depth of penetration

= MDPR). For water (1), we obtained a simple linear relationship between delivered impulse to wetted end of probe and measured MDPR, over a considerable temperature and pressure range, of the type:

$$MDPR = C_1 \text{ (Area)} - C_2 \qquad (1)$$

where Area = area under pulse-count energy spectrum curve,

i.e., Area = $\int_{E=0}^{E=\infty} N(E)\, dE$.

N(E) is number of pulses of energy E, per unit energy interval, as measured by electronic pulse counter, and dE is energy interval.

C_1 is amplitude constant directly relating Area and MDPR, and C_2 represents a "threshold" damage energy, as consistent with conventional cavitation damage expectations. It is encouraging that this correlation was linear with energy, since it is then consistent with the simplest of all possible and credible cavitation damage models.

The results for sodium are similar, as explained in the body of the report. However, the sodium measured damage rate results are surprising in that the classical expected curve (2,3) was found, i.e., damage decreased at both high and low temperature with intermediate maximum at ~380°C (=715°F)* except for an unexpected second increase at the highest temperature tested (550°F = 1022°F). This had not been found in our previous tests for the French AEC (2,3), but in that case the tests did not go above 500°C. Also, the material was a better high temperature material, 316 SS vs. 304 SS in present tests. We feel that the present high temperature increase is real, because it is virtually impossible mechanically for our

*maximum was at ~300°C from our previous tests (2,3).

rig to perform at higher than normal intensity at this extreme temperature. We feel that it is not an increase in mechanical cavitation fluid attack intensity which has been found, but rather the effect of significant decrease in the mechanical properties of 304 SS at this temperature, plus an increase of chemical effects at the high temperature. Thus the high-temperature increase should not be reflected in the pulse counts at this temperature. Presumably at the highest test temperature (550°C) these increasing normally secondary effects overcome the reduction in mechanical cavitation attack as temperature is increased above the maximum damage temperature.

II. Discussion of Results and Procedures

A. Sodium Damage Test Procedure

The sodium tests were concluded in our 20 kHz, 2 mil maximum double amplitude cavitation damage facility. It has been described in previous reports (1-3, eg). It is sealed so that an inert cover gas (argon) can be used, and tests at elevated pressure made (2 and 3 bar above p_v) to reduce required test time. For the sodium tests standard 1-hour runs were used to reduce required rig openings with concomittant additional contamination of sodium with oxygen. The specimens were attached and detached from the vibratory horn in an argon dry-box. They were cleaned before weighing with water and then thoroughly dried.

The MDPR data is of course directly derived from WLR (weight loss rate), which for the present tests is based on a single standard run duration of 1 hour at 1.5 mils horn double amplitude. Reduced horn amplitude (2.0 mil is conventional) was chosen, as explained in the earlier project reports (4,5) to reduce possible saturation of the counting circuit, and to maximize the likelihood of being able to maintain the same horn amplitude even up to the maximum temperature. However, it proved impossible, due to the complexities of the horn and driver design, to maintain even this reduced amplitude at all times. Hence for some of the highest temperature runs, a reduced horn amplitude was compensated by an increased test duration (as indicated in Table 1). The required increase of duration to maintain all runs directly comparable was computed according to the relation:

$$\text{WLR} \underset{\sim}{\propto} (\text{Amplitude})^{1.2} \qquad (2)$$

The "amplitude exponent" was determined from early tests under this project in water (4,5). While this correction procedure is not ideal, it was the only alternative possible, since time and money did not allow repeated runs or lengthy attempts at horn and driver modification to improve their operation. However, it is believed that the potential errors hereby introduced into the WLR data, do not affect the important results, particularly the rise in WLR at the maximum test temperature (550°C). We are confident of the validity of this statement, since the 550°C tests were made at 1.5 mils, and only 1 hour duration, i.e. "standard" conditions. Hence an error at this temperature on the high side, seems most improbable, and that is the point of major importance.

The temperatures tested range from 250 to 550°C at 50°C intervals (Table 1). Under all temperature conditions, tests were made at both 2 bar and 3 bar above vapor pressure (which is essentially zero for this purpose). Only one specimen was tested at each of these 14 conditions, due to limitations in time and money. Hence 14 successful sodium damage tests were actually made. This is a considerably greater scope of testing than was required by contract, since only 2 temperatures were specified there. For all test points, pulse counts were made over the desired frequency cut-off ranges.

The raw WLR vs temperature curves are included as Fig. 28.

B. <u>Sodium Pulse-Count Procedures</u>

The pulse count procedures in general were fully described in previous reports (1-5, eg). Wave-guide probes suitable for sodium were also used in the water tests so that an eventual direct comparison between water and sodium could be made. Hence the pulse count procedures used for sodium were exactly those previously described for water (1). Of course, the wave-guide probes are not ideal, and introduce unknown and not easily checkable signal distortion and attentuation. Direct submergence probes (such as the Kistler) would of course have been used had it not been for the very high temperature sodium requirements.

As discovered from our water tests, increased low-frequency cut-off frequency improves markedly the correlation between integrated pulse-count energy (area under curve of N(E) vs E).

For the water tests, only 40 and 60 kHz low frequency cut-off settings were used. An apparently remarkably good correlation with measured damage was achieved for the 60 kHz cut-off (Fig. 53 of Ref. 1) but mostly random scatter at 40 kHz. This is not unexpected, since the vibratory horn 20 kHz input signal could well produce a significant contribution at 40 kHz, but probably much less at 60. In addition W-ARD using a venturi* indicates a probe resonant behavior at 40 kHz. However, we can see no logical justification for such a phenomenon, since resonant frequency of wave-guide rod is much too low, and that of crystal itself is much too high. In any case, guided by these previous results, we altered our procedure for sodium. We have included again 40 and 60 kHz cut-offs, to maximize opportunity of direct comparison with our water, and also the W-ARD sodium tests. However, we have gone to the limits of our presently available electronic equipment by including frequency cut-off settings of 70, 80, and 90 kHz. Again it appears that within these limits the higher the cut-off frequency the better the pulse count data, and the better the correlation with measured damage rates. The pulse count raw data plots are presented as Figs. 1-21.

As explained in ref. 1 the area under these spectrum curves is ideally proportional to impulse or energy delivered to the probe by the collapsing bubbles. Under a newly commenced contract with ONR we are attempting to make a direct calibration between input received and pulse-count spectrum area in a bench-type probe calibration rig. However, no definitive results will be available immediately.

*rather than vibratory horn.

Figures 22-27 show the pulse-count areas plotted against sodium temperature. A considerable similarity to the analogous MDPR vs. temperature curves will be noted. All the pulse-count areas and corresponding MDPR(s) are listed in Table 1.

III. Discussion and Analysis of Results

A. General

As already mentioned Figures 1-21, show the raw pulse count data and the areas beneath the spectrum curves. The spectrum areas are also listed in Table 1.

Fig.22-27 show the variations of pulse-count spectrum areas as a function of sodium test temperature.

Fig. 28 shows the variation of measured MDPR with sodium temperature, and these data are listed in Table 1.

Fig.29-33 show the eventual correlations between smoothed MDPR (all pressure and temperature conditions included in the same graph) and pulse-count area spectra.

MDPR data taken directly from the 'smoothed curves' has been used to correlate with the measured pulse-count spectra, rather than the "raw data" points. It is believed that the greatest benefit for the present purpose will result from the use of the smoothed damage data, since variations from the smoothed curve, whose general shape is well known from numerous previous tests, would most probably be substantially eliminated by additional sodium damage testing, which, however, is not possible due to time and funding limitations. The smoothed erosion curves assume a continued fall of erosion rate with increased temperature, since it is believed that the observed rise at maximum temperature is the result of reduced mechanical material properties and increased corrosion, and hence is not relevent to the present situation, and should not be reflected by the pulse counts, which of course are not sensitive to these effects.

The effects of the different cut-off frequencies are shown by comparison of the different figures.

The best fit curves between pulse count spectrum areas and MDPR are shown on each curve along with the standard error.

B. Specific Results

1. General

Figures 29-33 show the correlations obtained at different cut-off frequencies between the smoothed MDPR curves and the measured pulse count energy areas. Linear fits for this data are clearly not useful, since they would indicate zero cavitation damage under conditions of substantial pulse count. Therefore, exponential curves have been used, indicating an increasing rate of erosion for increased pulse count area according to an exponential relations as below, where the best values for "n" are listed in Table 2, for the different cut-off frequencies.

$$MDPR = C_1 \ (Area)^n \qquad \text{------} \qquad (2)$$

2. Comparison with Water Results

Our earlier water results previously reported (1) indicated a linear fit for the water data, i.e., n = 1. However, a comparison of the water MDPR values with those for sodium, indicates that the water tests are in general "less intense" than the sodium tests (identical test facility parameters except temperature) by a factor of at least 2. If this difference in test intensity between sodium and water tests is taken into account, the apparent inconsistency between the sodium and water tests vanishes in that the lower intensity portion may well be linear, becoming exponential at higher levels of intensity. This supposition is illustrated by Fig. 34.

The actual factor between water and sodium intensities under identical test conditions is probably greater still by at least 50% because of the difference in test methods employed for the two liquids. Whereas the water tests included the actual generation of the classical S-shaped MDP vs. time curves, so that the $MDPR_{max}$ could be evaluated accurately, the sodium tests were single-point values (1 hour) only, due to limitations of time and funding. Thus the sodium tests provide only an average MDPR, which is certain to be substantially less than the maximum. We estimate this difference to be at least 50%, i.e., $MDPR_{max} \gtrsim 3/2\ MDPR_{aver}$.

Figure 34 shows our best estimates of the comparison between water and sodium and the overall pulse-count spectra vs. $MDPR_{max}$ curves. The sodium MDPR values have been increased by the above mentioned factor of 3/2. The smoothed exponential curves for the sodium data are shown on these curves along with the presumed linear portion (from ref. 1) for the water tests. The different figures apply to the different cut-off frequencies for the pulse counts. It is our opinion that the higher frequency results (to 90 kHz) are likely to be the more accurate since the suppression of extraneous inputs is then most complete.

Unfortunately the validity of Figure 34 cannot be more firmly established at this time without the obtaining of lower intensity sodium data, as well as further reenforcing of the water pulse counts, which are in fact in the low intensity MDPR range. At this point we do not feel justified in directly comparing the magnitudes of pulse count areas for water and sodium due to unavoidable changes in probe performance which occurred after the water tests. Thus additional data at the low intensity end would be highly desirable.

III. Conclusions

The major conclusions which can be drawn from the work here covered are as follows.

1. A reasonable engineering correlation (Fig. 34 , e.g.) between bubble collapse pulse count energy spectra and measured volume loss rates for both sodium and water, over their respective temperature ranges of interest, and for suppression pressures of 2 and 3 bar in our 20 kHz, 1.5 mil vibratory facility, on 304 SS, has been obtained. The water data and sodium data appear to be correlated by the same curve, although additional low intensity data is required to fully verify the match between sodium and water.

2. Further work, now in progress under a related ONR contract, is required to reduce the pulse count energy spectra to absolute (rather than relative) values so that these results could be applied to other systems such as, eg., a venturi or other flowing device, and other materials, for à priori damage prediction. The capability for such prediction is of course the ultimate aim of this study, and now appears not too remote.

3. A direct comparison between water and sodium damage rates in the same vibratory test facility with identical test parameters (except temperatures, which of course covered the individual ranges of interest) and with the same test material (304 SS) indicates that sodium under such conditions is

approximately 3 x as damaging as water. Of course, this ratio may not apply to other test conditions or materials. However, the completion of the development of the predicting technique here used would allow the immediate and easy determination of that ratio for any particular flow system.

4. The maximum damage temperature for the sodium under present test conditions upon 304 SS, at either test suppression pressure (2 or 3 bar) is ~ 380°C* (716°F). This maximum damage temperature is somewhat higher (~380°C vs. ~300°C) than we had previously found (2,3) for 316 SS. This difference may be attributed partially to the reduced high temperature strength of 304 vs. 316.

5. Present tests indicated an increase in damage for the maximum temperature tested (550°C = 1022°F), although it is almost certain that the mechanical component of cavitation attack would be strongly reduced for increasing temperature in this range. Also, the presumed reduction in mechanical cavitation attack was supported by a decrease in pulse count energy at this temperature. Therefore, we believe that the increased damage at maximum temperature is attributed to a significant decrease in material mechanical properties, and an increase in corrosive effects, at this temperature.

*It is generally expected that the maximum damage temperature will increase with pressure, but the difference between 2 and 3 bar was not great.

Bibliography

1. F.G. Hammitt, J.B. Hwang, G. Chammas, M.K. De, A. El Hasrouni, J.A. Faust, A. Seskaini, "Progress Report No. 3, Argonne National Laboratory," UMICH Report No. 013503-3-PR, Feb. 1975.
2. F.G. Hammitt, N.R. Bhatt, "Sodium Cavitation Damage Tests in Vibratory Facility," 1975 ASME Polyphase Flow Forum, p. 22-25.
3. F.G. Hammitt, N.R. Bhatt, "Sodium Cavitation Damage Tests in Vibratory Facility - Temperature and Pressure Effects," Proc. 5th Conf. on Fluid Machinery. Budapest, Sept. 1975, p. 393-401.
4. F.G. Hammitt, N.R. Bhatt, O.S.M. Ahmed, K. Yue, "Vibratory-Flowing System Correlation Study in Sodium," UMICH Report No. 013503-1-PR, April 1975.
5. F.G. Hammitt, "Progress Report No. 2, Argonne National Laboratory," UMICH Report No. 013503-2-PR, Nov. 1975.

Temp °C/°F	Press. (atm.)	WLR mg/hr.	$MDPR_{act}$ microinch-hr.	WLR (smoothed)	MDPR (smoothed)	Area for Curves 40 kHZ	60 kHz	70 kHz	80 kHz	90 kHz
250/	2	113	3570	113	3555	7060	5025			
480	3	43	1360	40	1258	5790	1644			
300/	2	153	4820	138	4342	1925	1160	670	360	250
572	3	189	5960	138	4341	3100	890	730	860	340
350/	2	136	4270	160	5033	1205	443	215	90	83
663	3	170	5350	195	6135	8323	3340			800
400/	2	113	3545	160	5033	3153	2295	1743	1403	1033
752	3			210	6606	10340	9273	1773	898	973
450/	2	155	4830	135	4247	2430	1785	1088	1138	610
840	3	231	7270	175	5505					
500/932	2	140	4380	110	3460	763	458	323	100	155
	3	55	1705	75	2360					
550/	2	220	6890	80	2517					1855
/1022	3	75	2370			2293	1250	1250	610	553

Table 1

Test Parameters and Results

Table 2

Exponent Values for Area vs. MDPR Curves

$$MDPR = C_1 (Area)^n$$

Cutoff Frequency	n
40 kHz	4.16
60 kHz	4.22
70 kHz	5.18
80 kHz	6.36
90 kHz	4.77
Aver.	4.94

FIGS 1 - 21

KEY

	3atm - 40 KHz	(1)
	2atm - 40 KHz	(2)
	3atm - 60 KHz	(3)
	2atm - 60 KHz	(4)
	3atm - 70 KHz	(5)
	2atm - 70 KHz	(6)
	3atm - 80 KHz	(7)
	2atm - 80 KHz	(8)
	3atm - 90 KHz	(9)
	2atm - 90 KHz	(10)

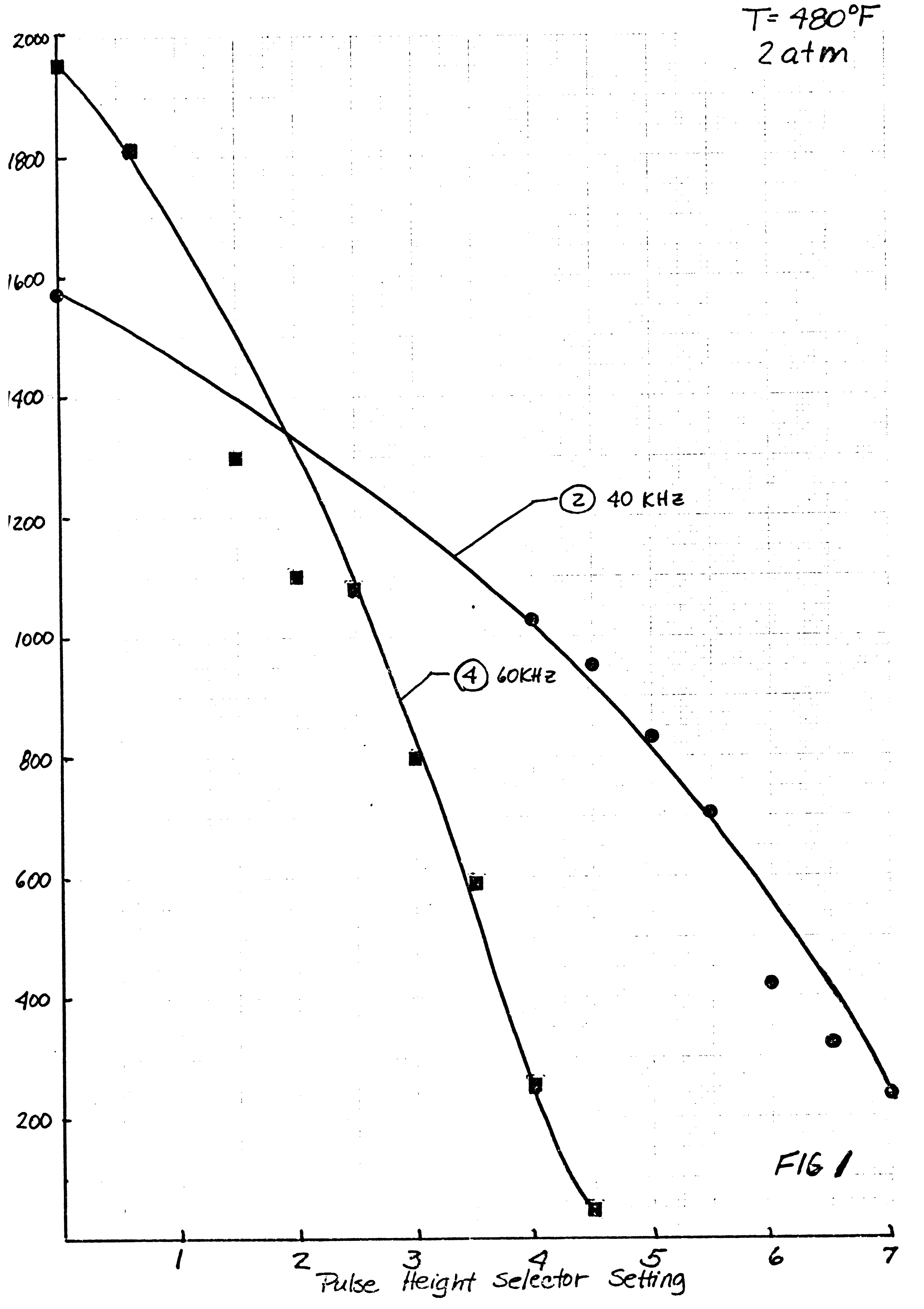

T= 480°F
2 atm
2000
1800
1600
1400
1200
1000
800
600
400
200
(2) 40 KHz
(4) 60KHz
1
2
3
4
5
6
7
Pulse Height Selector Setting

FIG 1

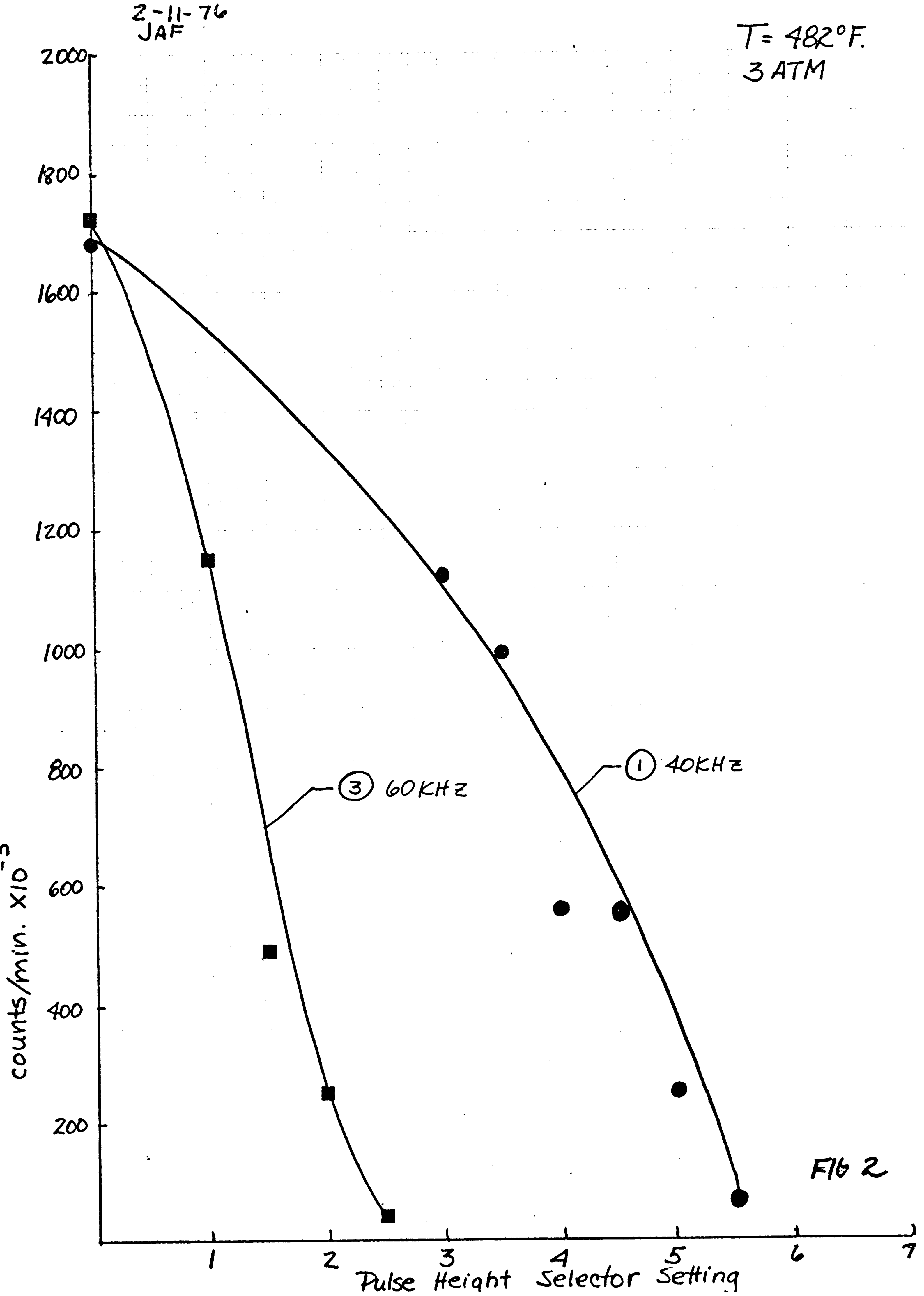
2-11-76
JAF
T = 482°F.
3 ATM
2000
1800
1600
1400
1200
1000
800
600
400
200
counts/min. X10^-3
③ 60KHz
① 40KHz
1
2
3
4
5
6
7
Pulse Height Selector Setting

FIG 2

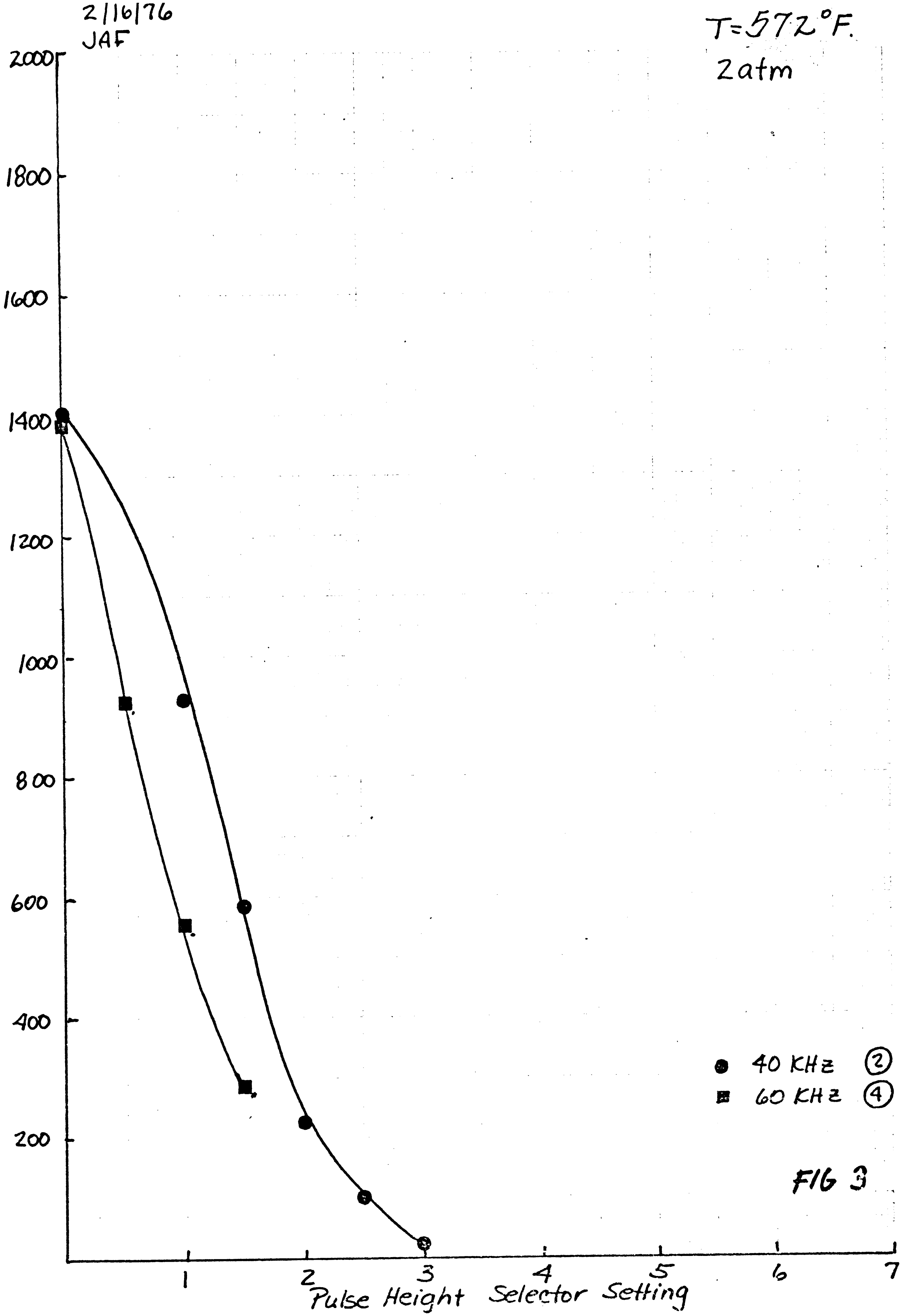
2/16/76
JAF
T=572°F.
2atm
2000
1800
1600
1400
1200
1000
800
600
400
200
40 KHz ②
60 KHz ④
1
2
3
4
5
6
7
Pulse Height Selector Setting

FIG 3

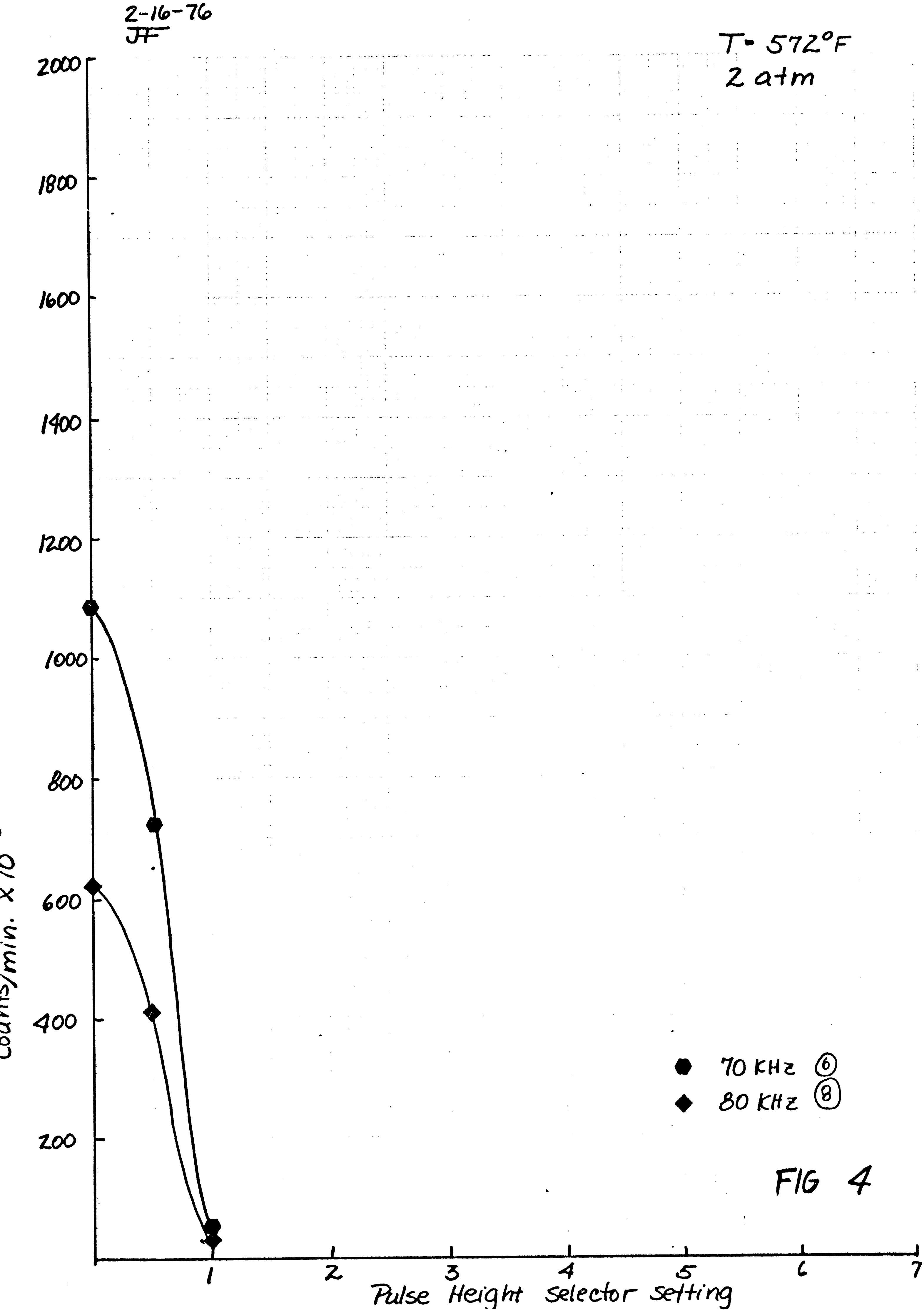
2-16-76
JF
T= 572°F
2 atm
2000
1800
1600
1400
1200
1000
800
600
400
200
Counts/min. x 10
70 KHz (6)
80 KHz (8)
1
2
3
4
5
6
7
Pulse Height selector setting

FIG 4

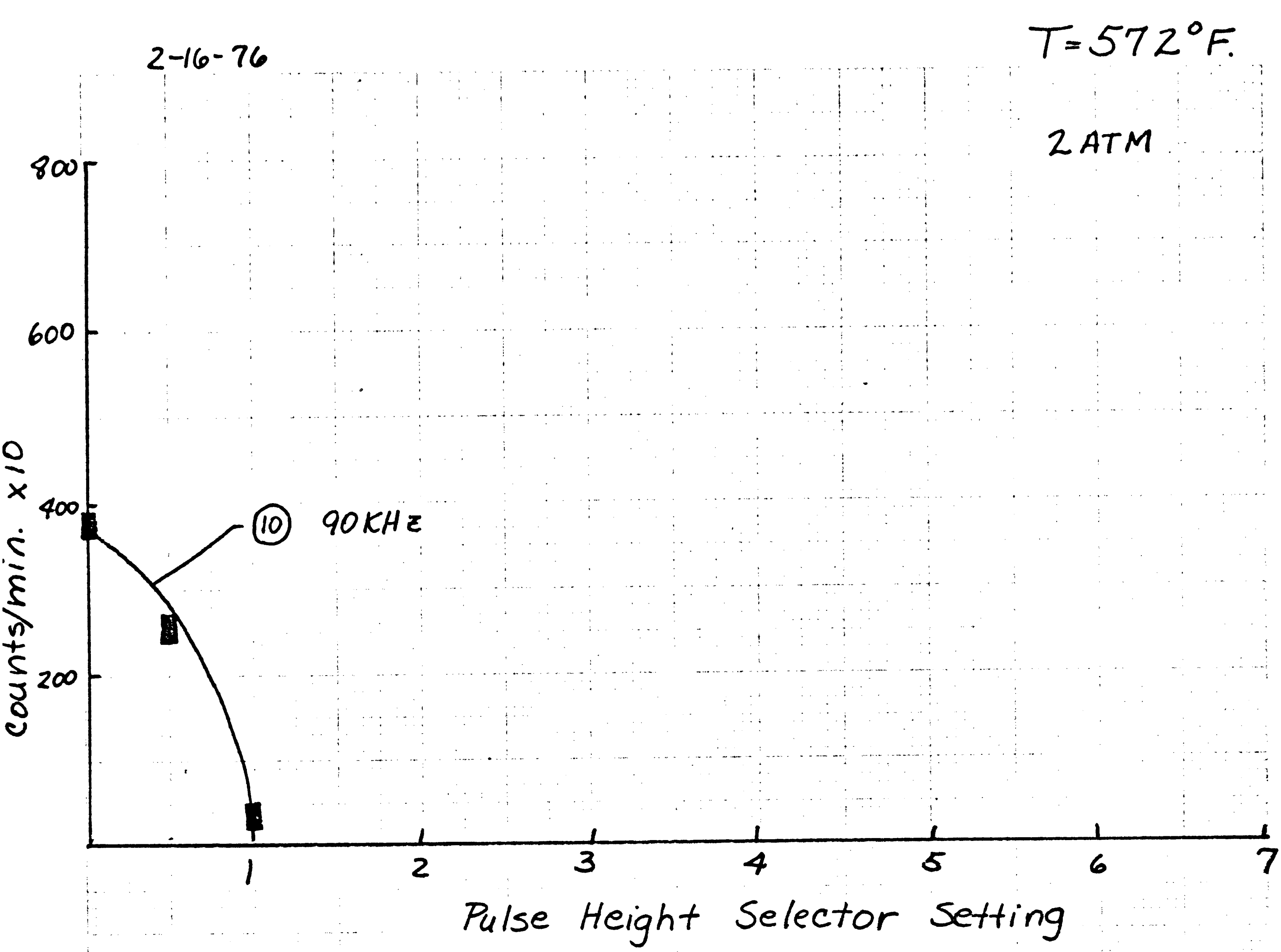
2-16-76
T=572°F.
2ATM
800
600
400
200
counts/min. x10
(10) 90KHz
1
2
3
4
5
6
7
Pulse Height Selector Setting

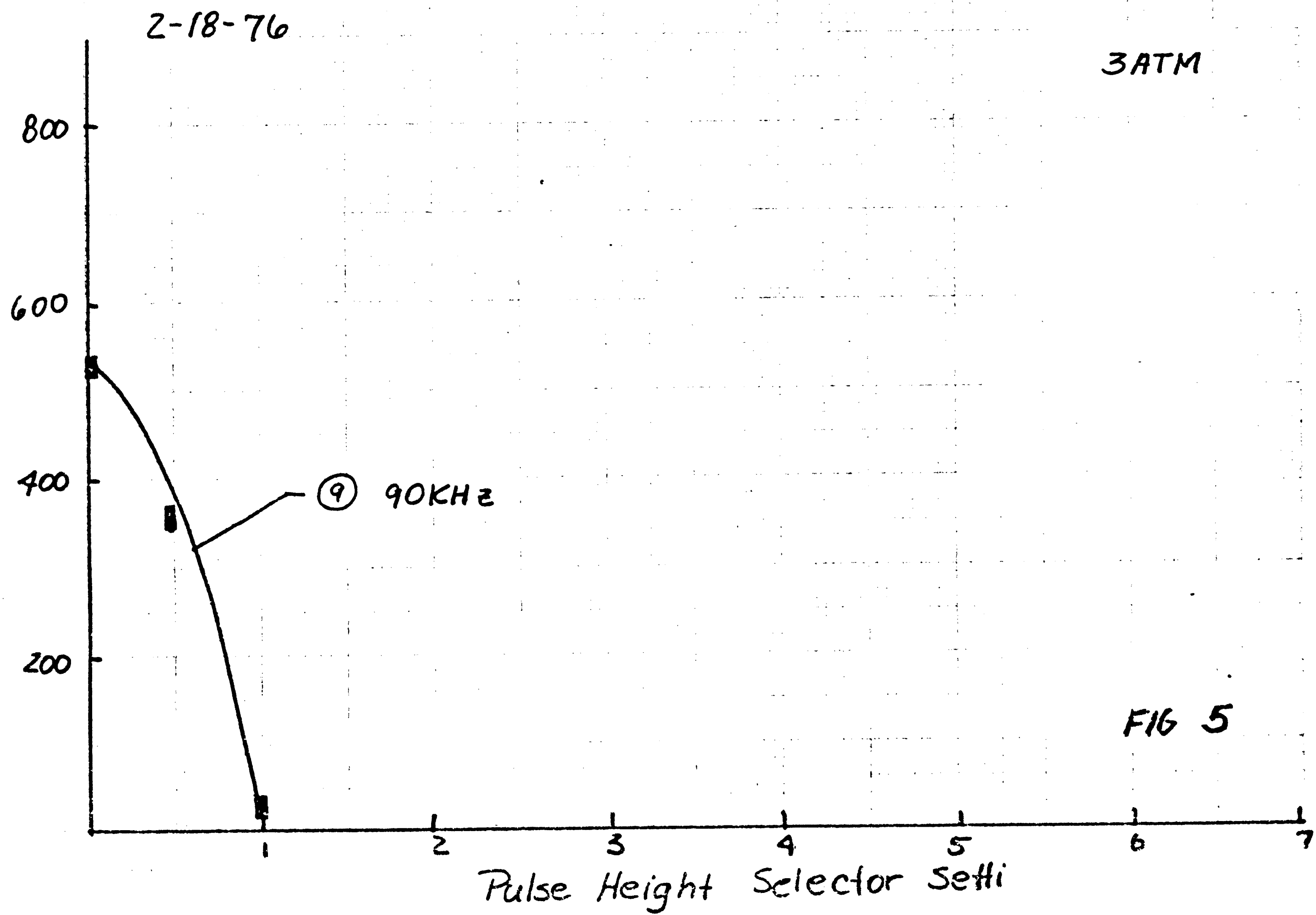
2-18-76
3ATM
800
600
400
200
(9) 90KHz
1
2
3
4
5
6
7
Pulse Height Selector Setti

FIG 5

2-8-76
J.A.F.

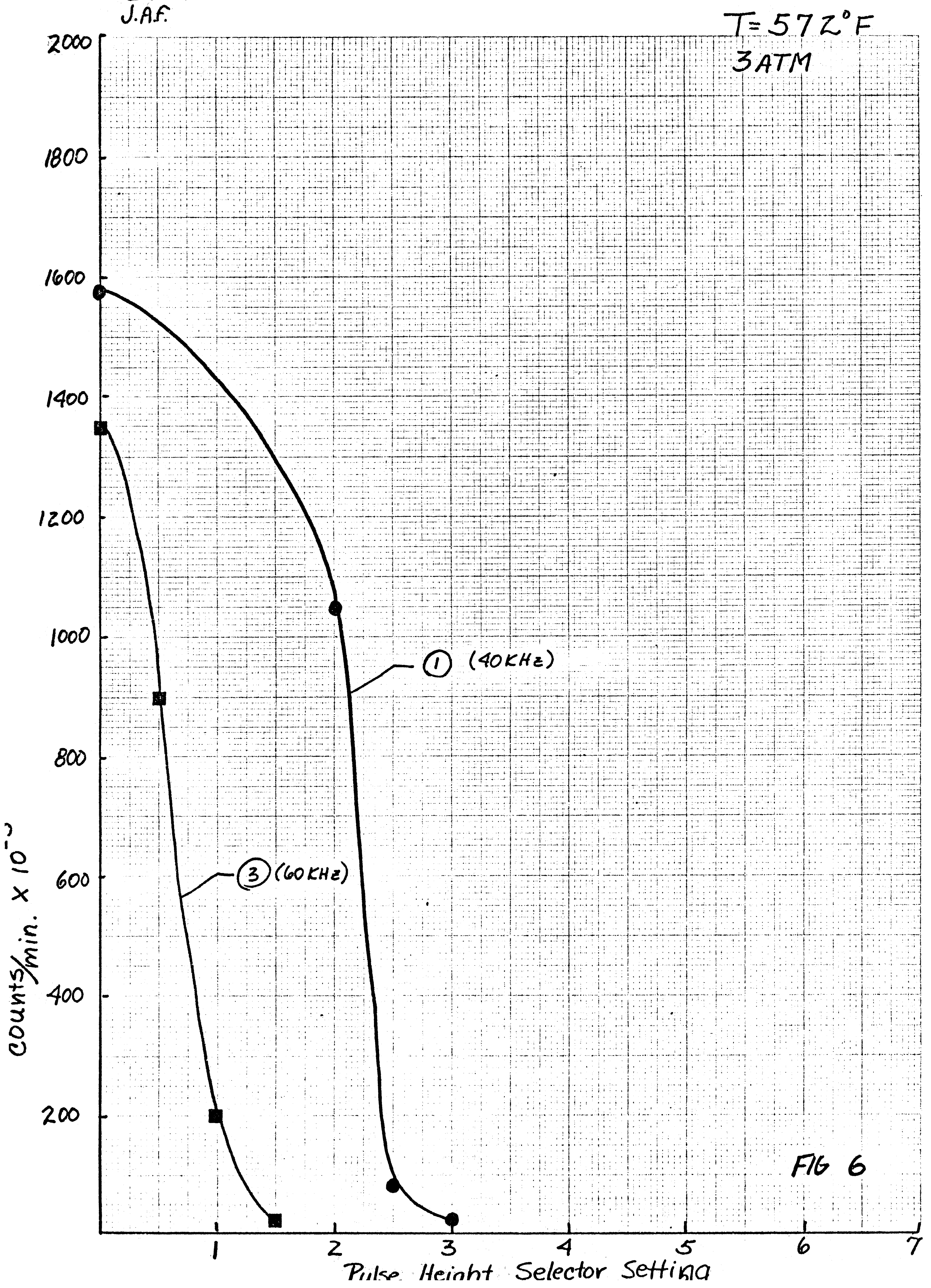

FIG 6

2-18-76
JAF

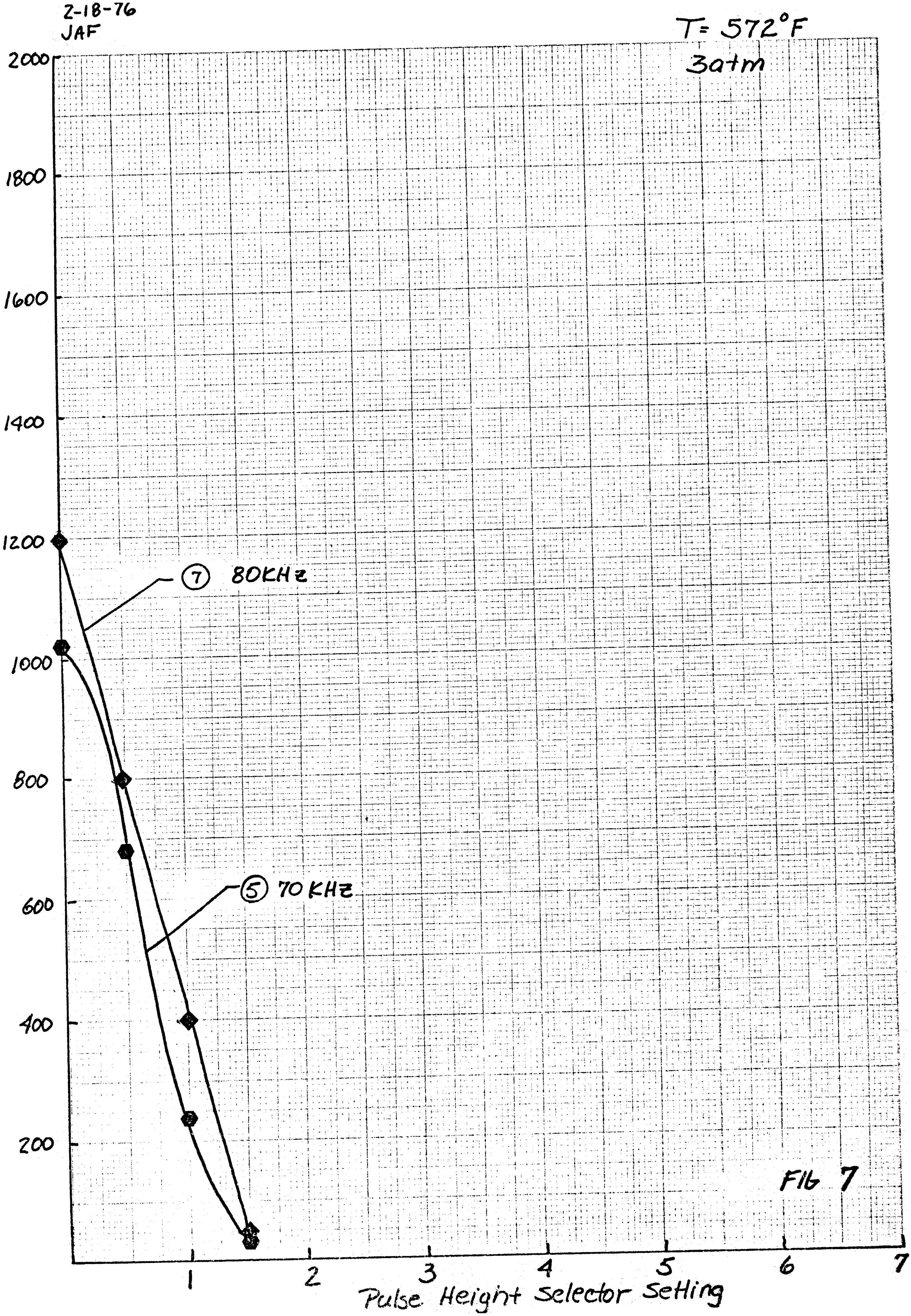

FIG 7

2/25/76
JAF

T = 662°F

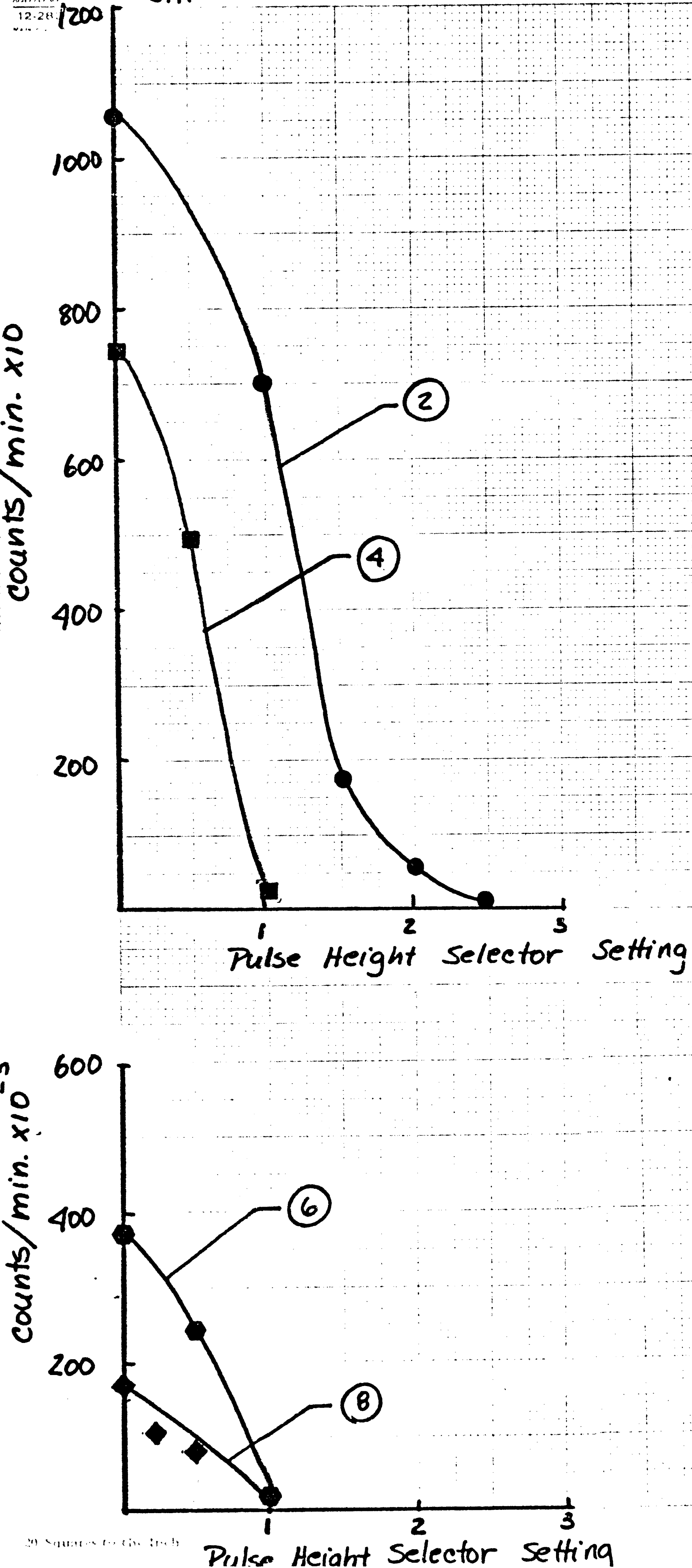

FIG 8

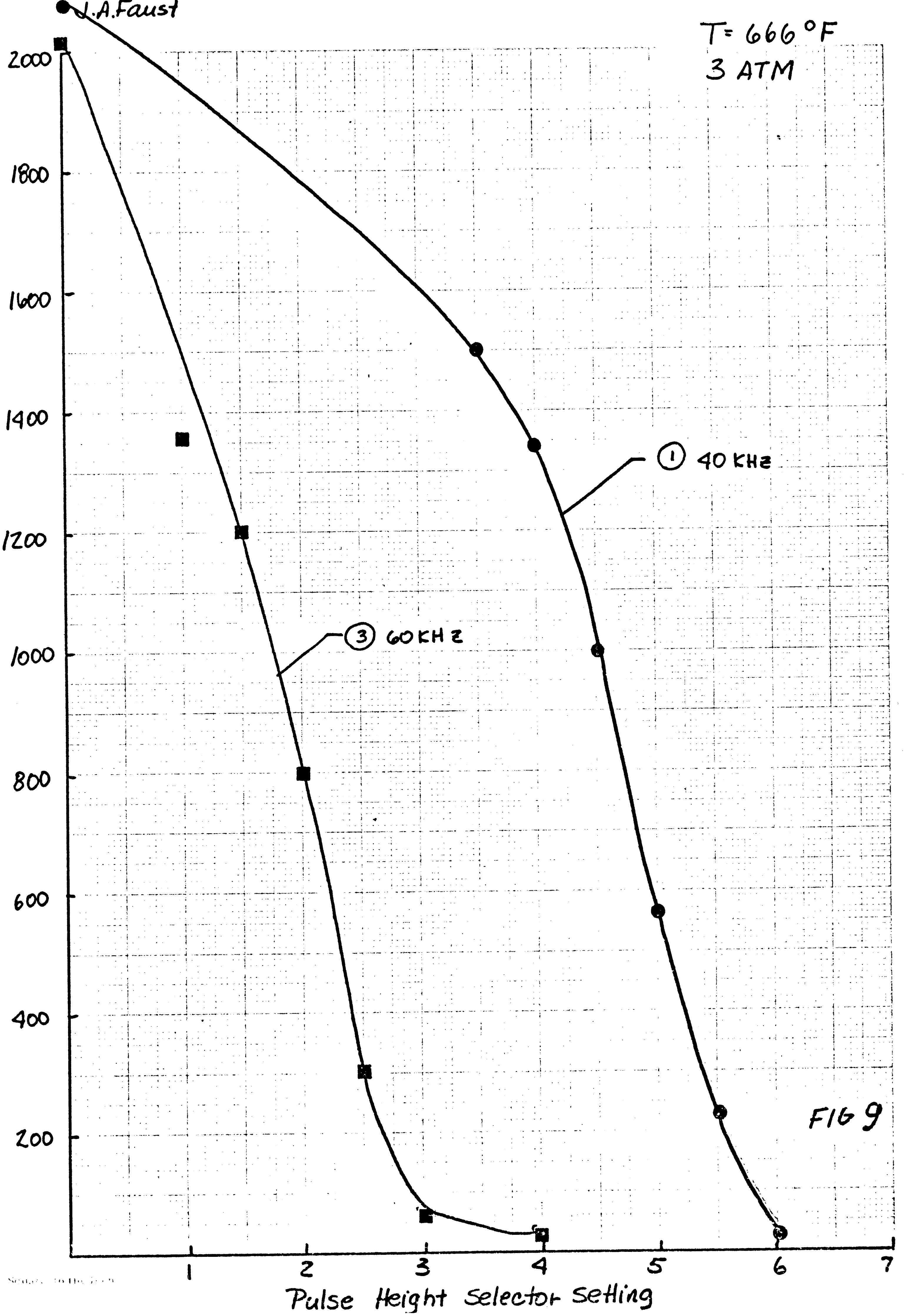
J.A.Faust
T= 666 °F
3 ATM
2000
1800
1600
1400
1200
1000
800
600
400
200
① 40 KHz
③ 60 KHz
1
2
3
4
5
6
7
Pulse Height Selector Setting

FIG 9

J.A. FAUST

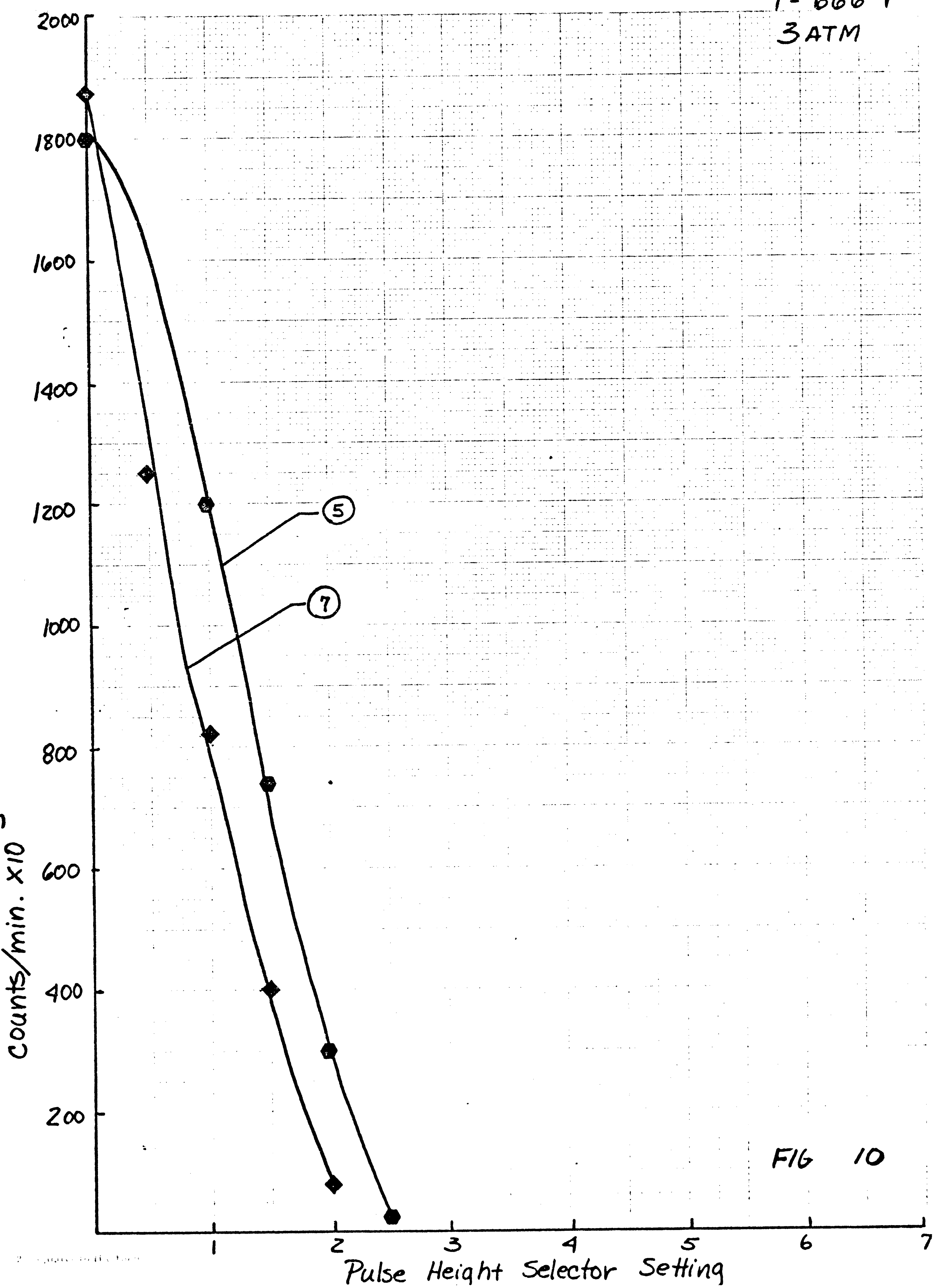

FIG 10

JAF

JAF

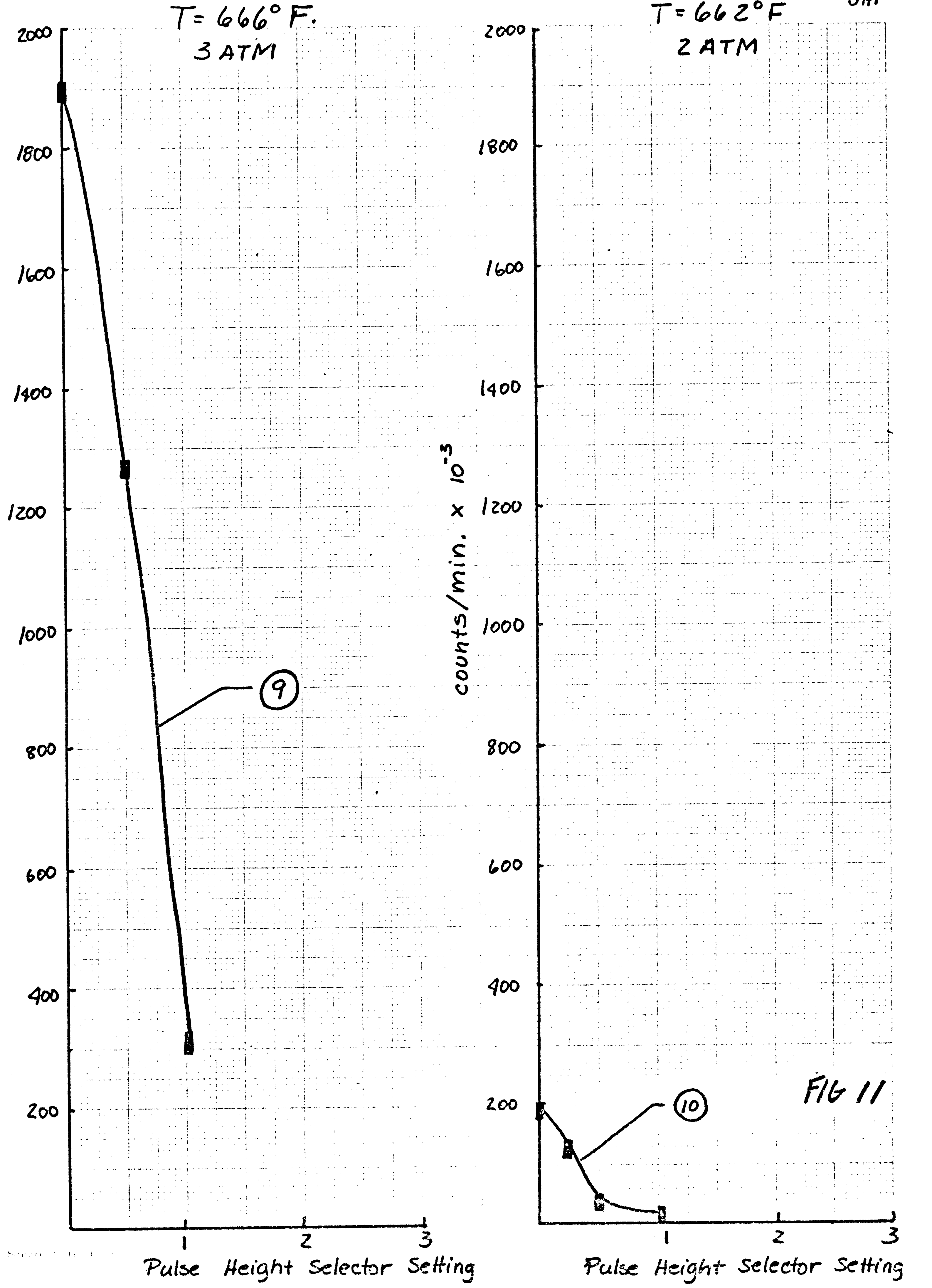

FIG 11

2-27-76
JAF

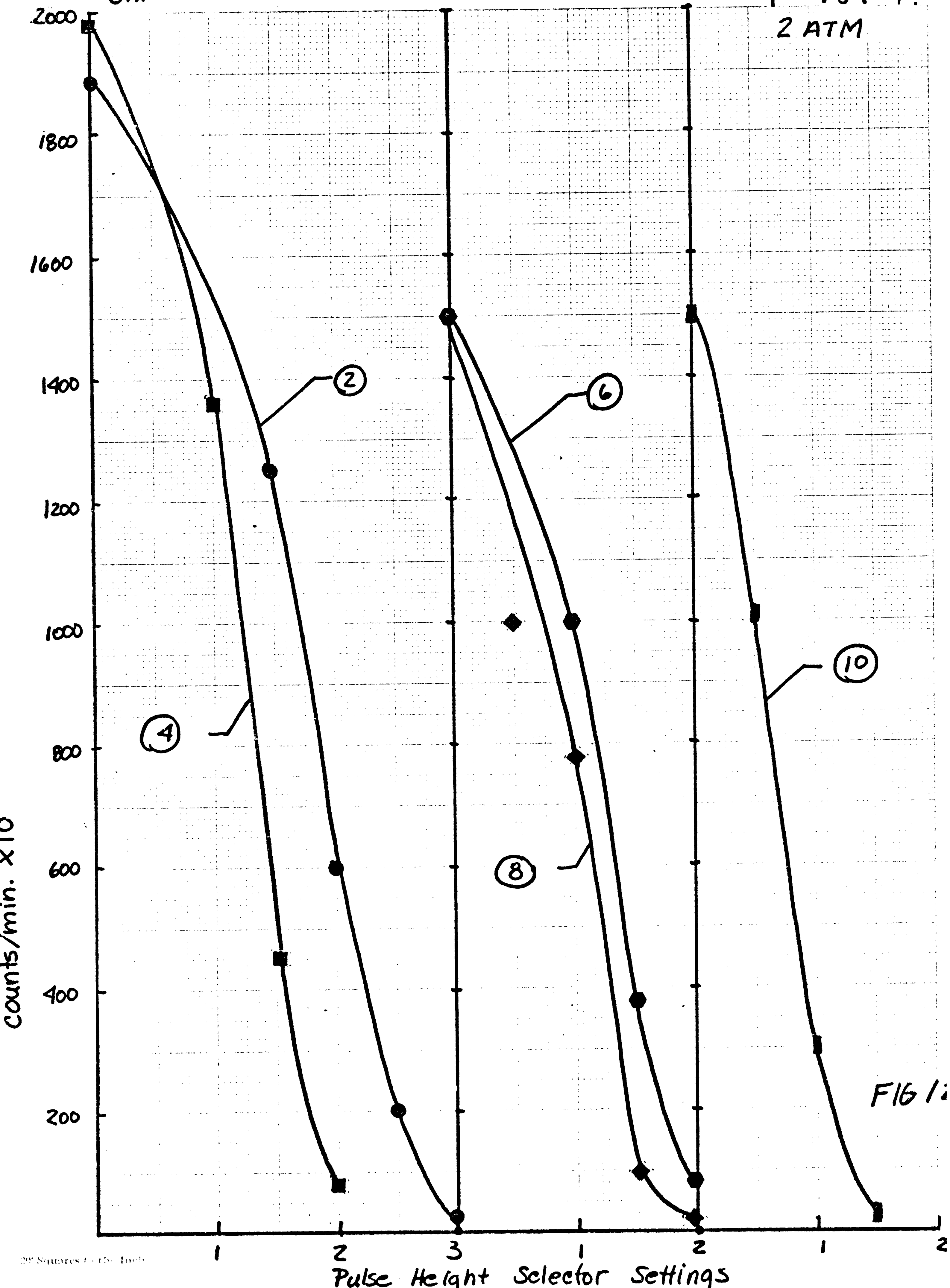

FIG 1

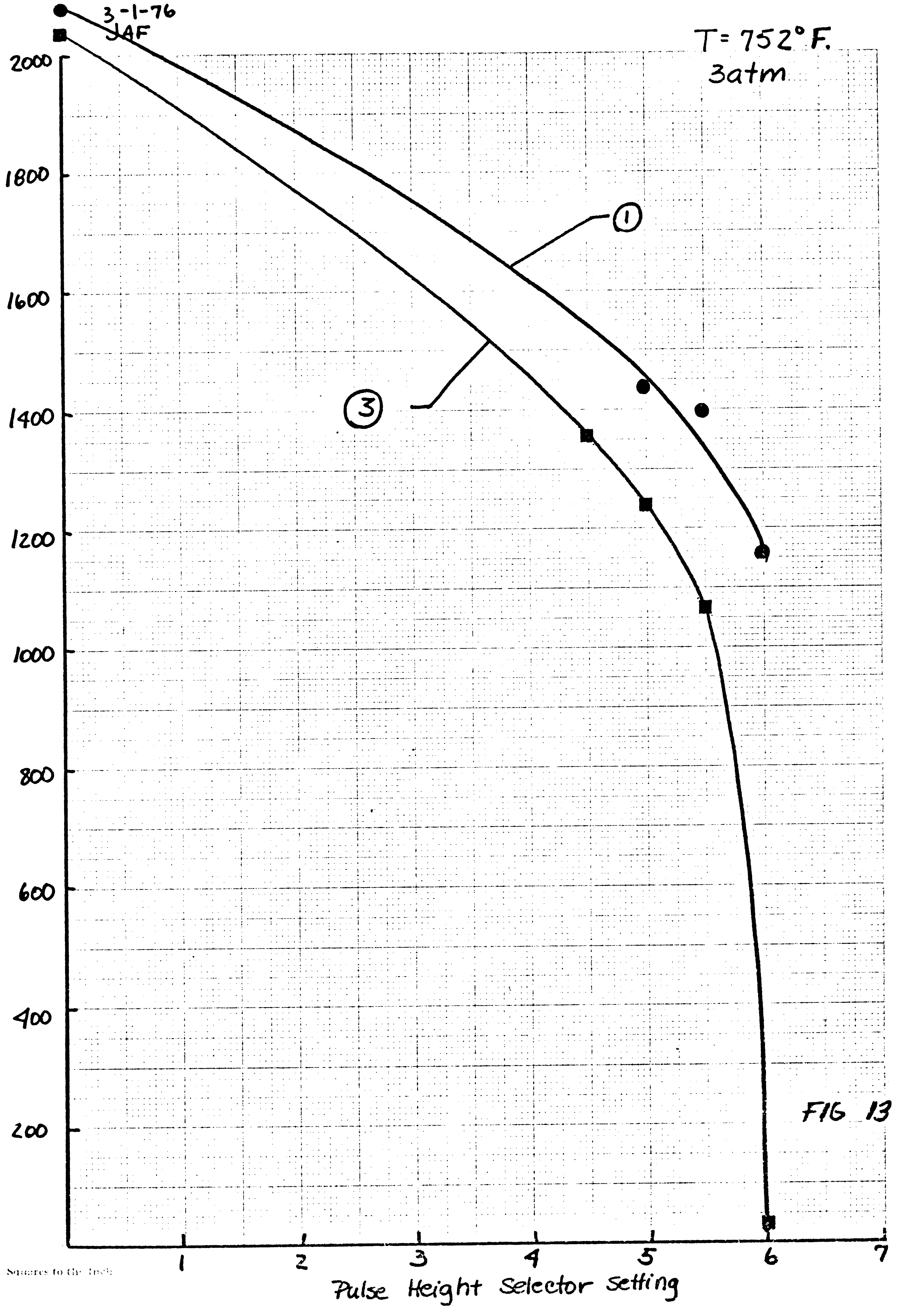
3-1-76
JAF
T = 752° F.
3atm
2000
1800
1600
1400
1200
1000
800
600
400
200
1
2
3
4
5
6
7
①
③
Pulse Height Selector Setting
Squares to the Inch

FIG 13

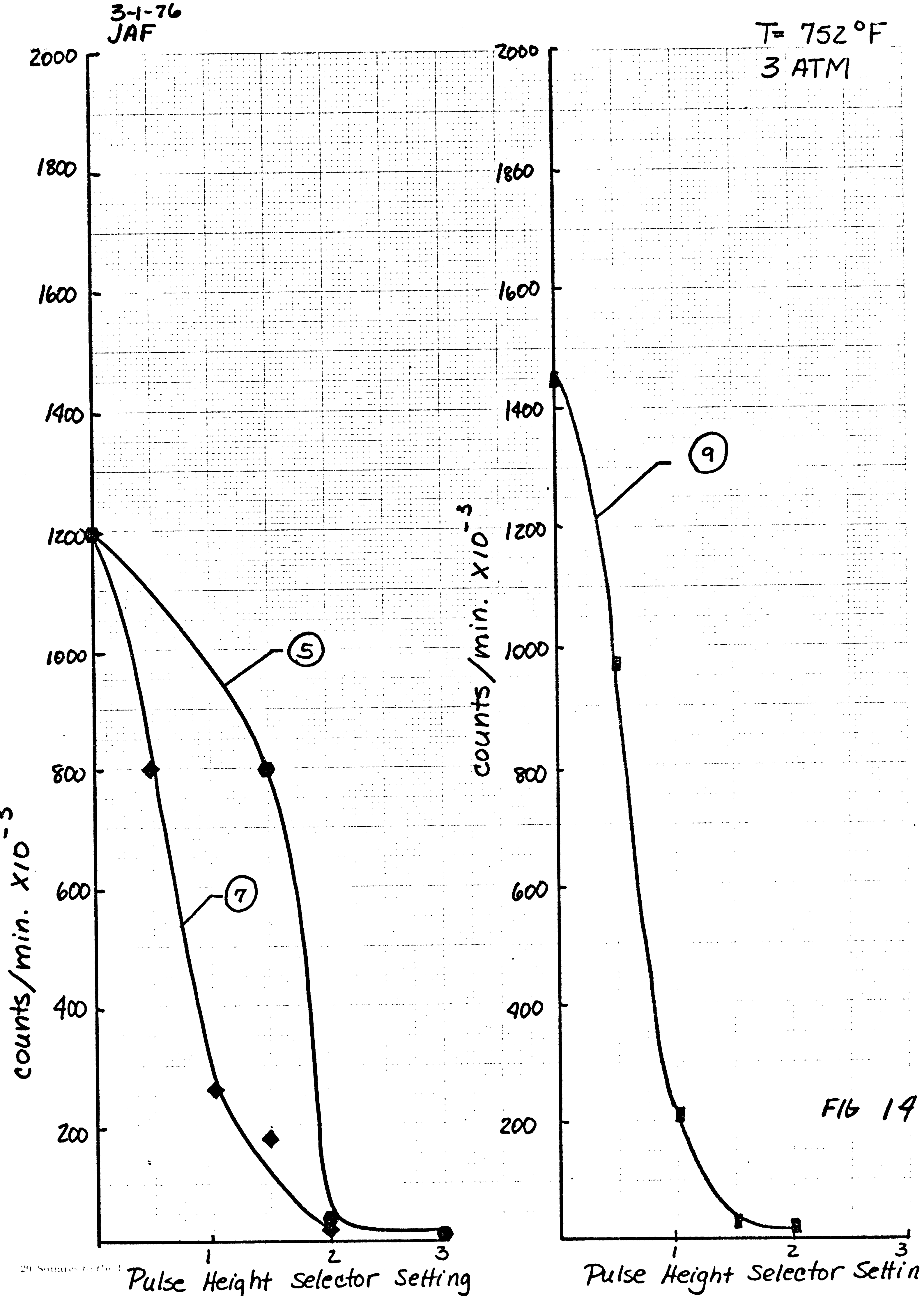
3-1-76
JAF
T= 752°F
3 ATM
2000
1800
1600
1400
1200
1000
800
600
400
200
counts/min. X10^-3
5
7
9
1
2
3
Pulse Height selector Setting
Pulse Height Selector Settin

FIG 14

4-1-76
J.A. Faust

T= 842°F
2 ATM

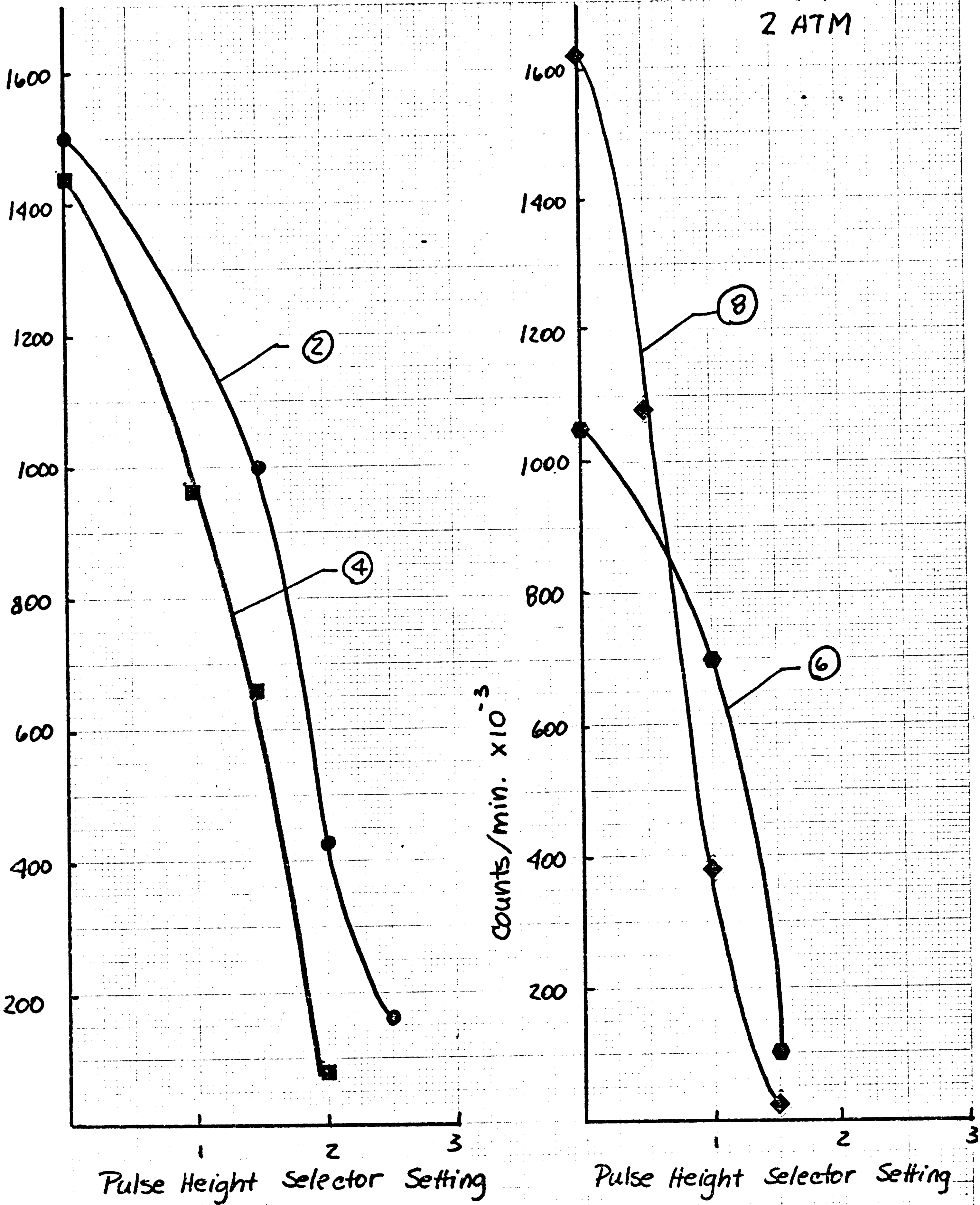

FIG 15

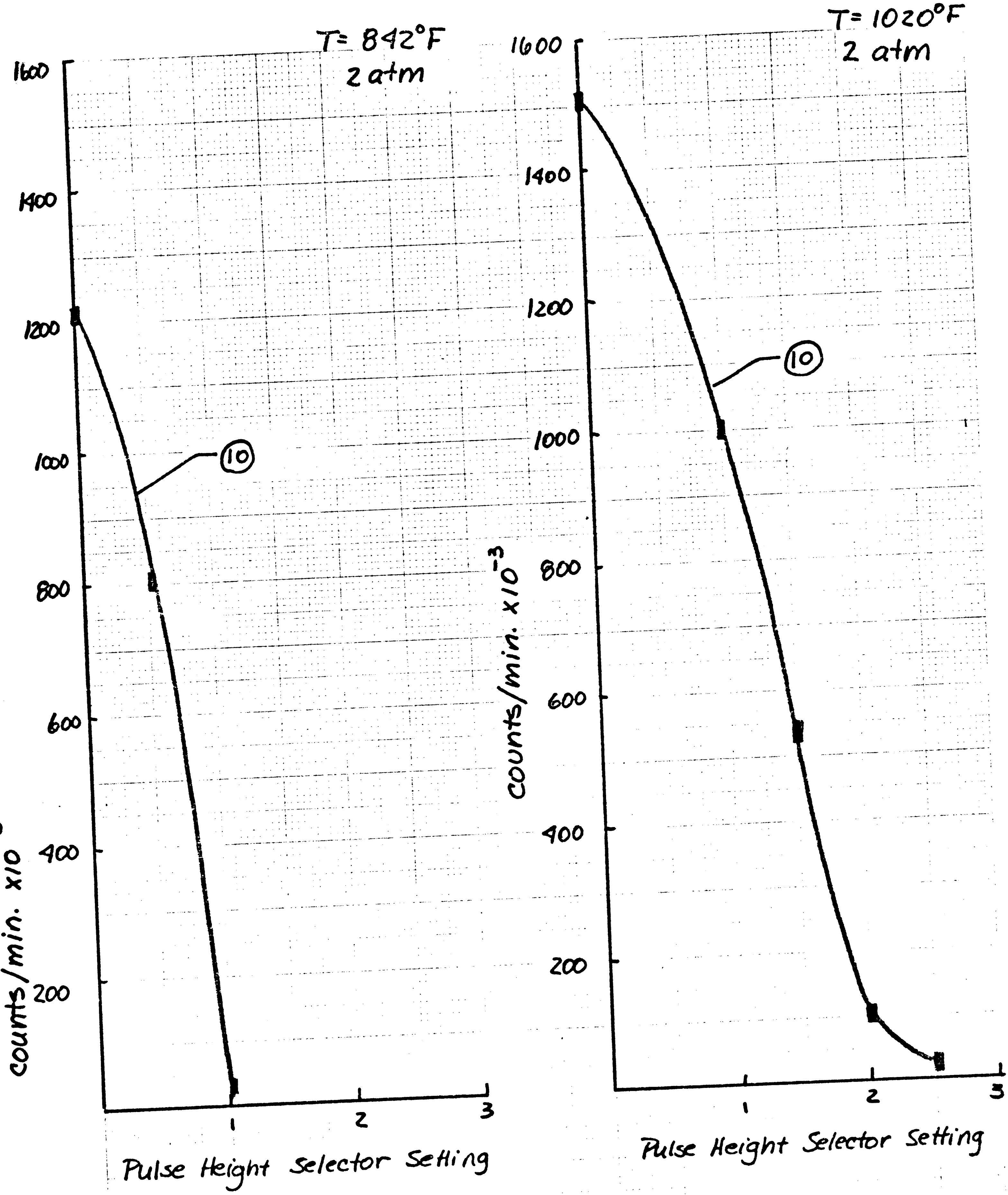

T= 842°F
2 atm
1600
1400
1200
1000
800
600
400
200
counts/min. x10⁻³
10
1
2
3
Pulse Height Selector Setting
T= 1020°F
2 atm
1600
1400
1200
1000
800
600
400
200
counts/min. x10⁻³
10
1
2
3
Pulse Height Selector Setting

FIG 16

4-1-76
Judit Faust

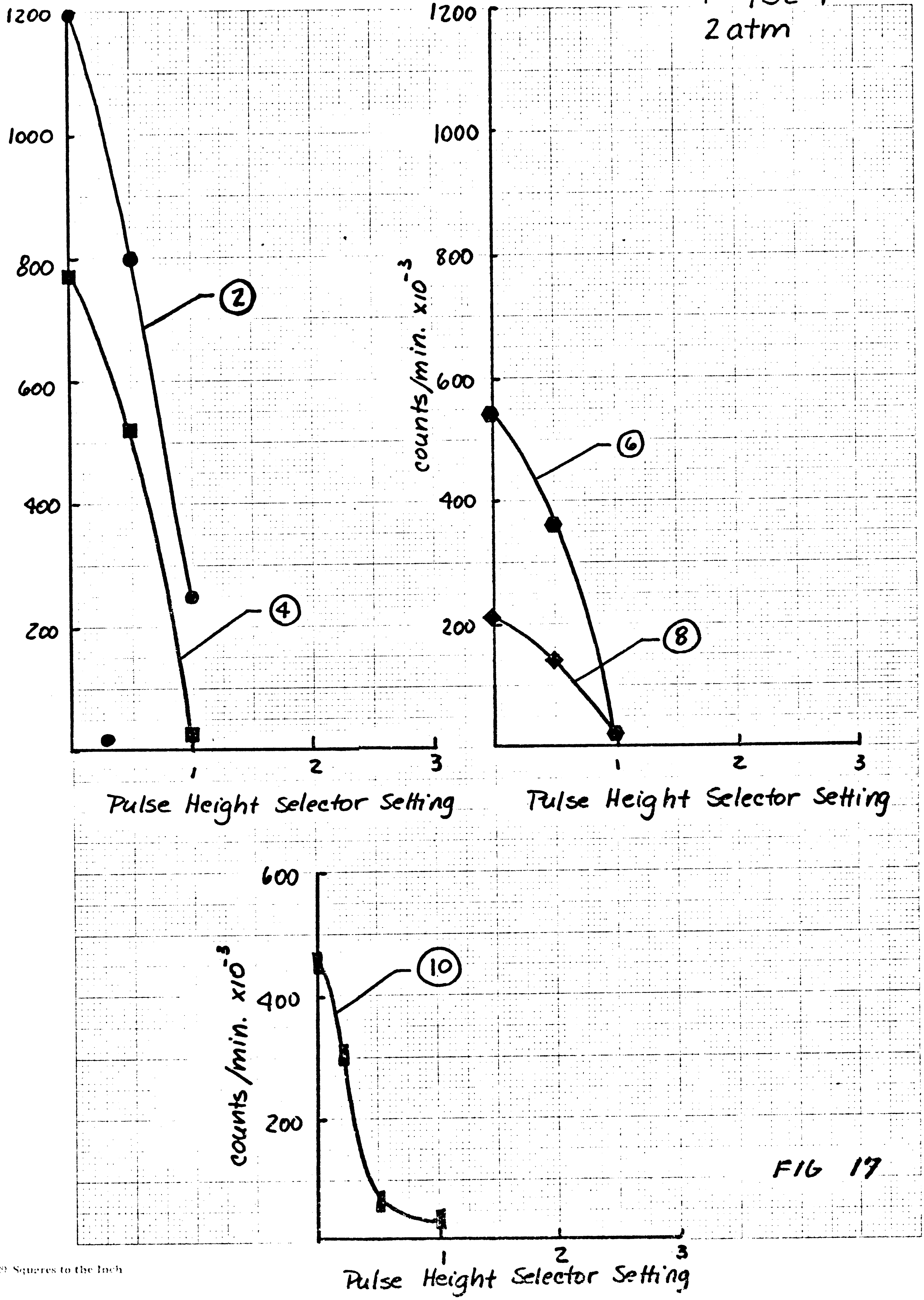

FIG 17

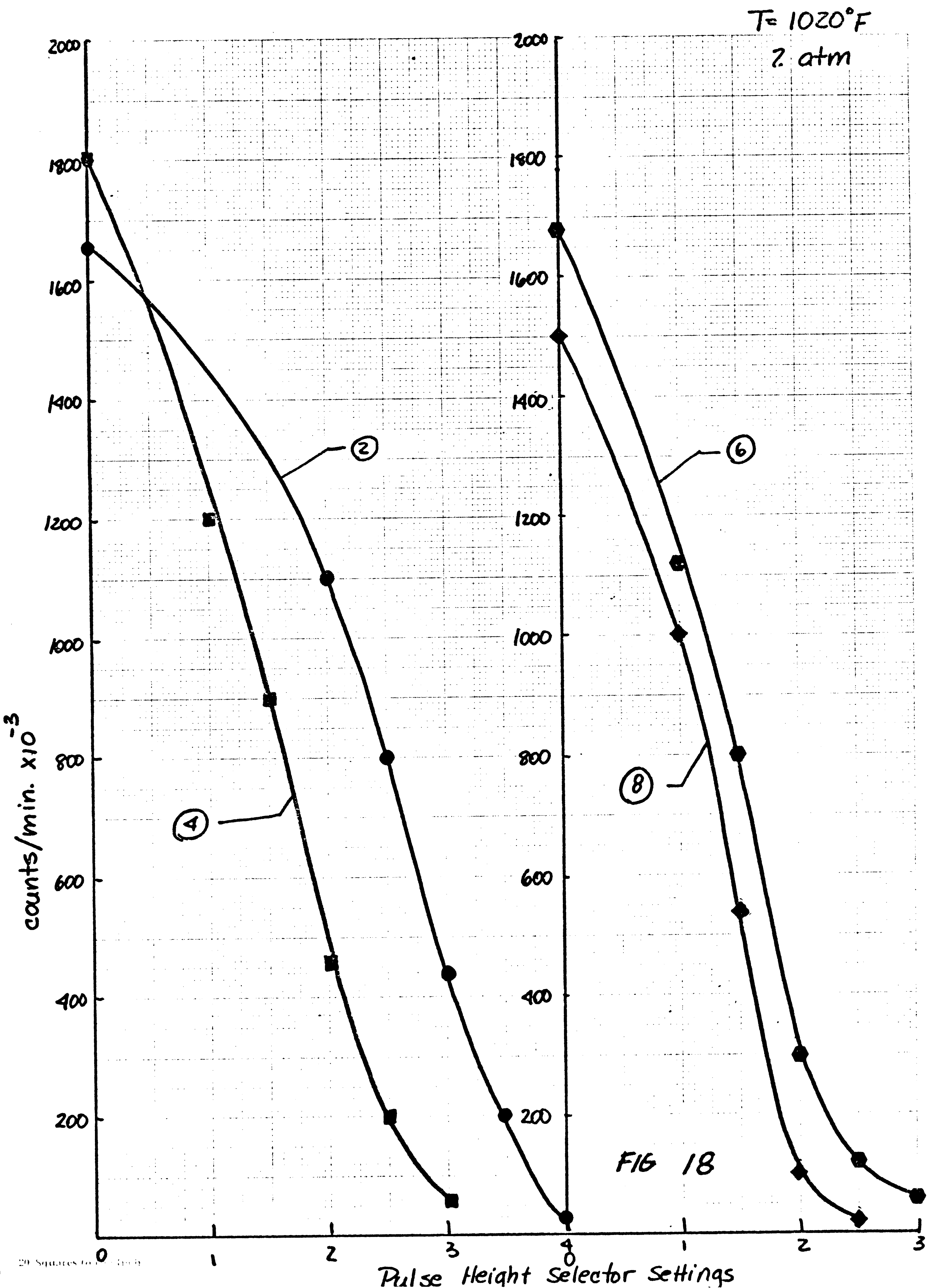

T= 1020°F
2 atm
counts/min. x10^-3
2000
1800
1600
1400
1200
1000
800
600
400
200
2
4
6
8
0
1
2
3
4
Pulse Height Selector Settings

FIG 18

S. Barber 12 April, 1976

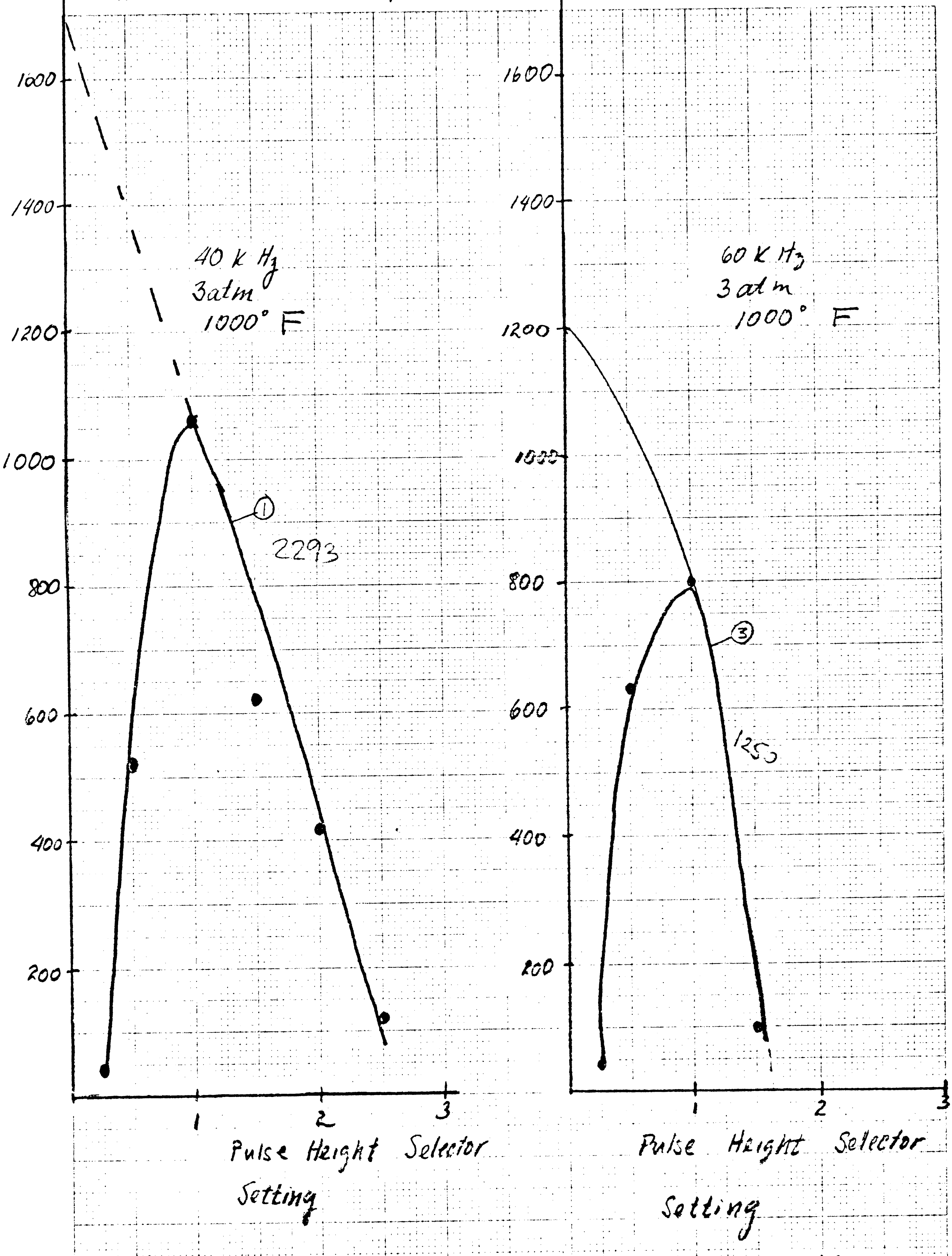

FIG 19

S. BARBER 12 April

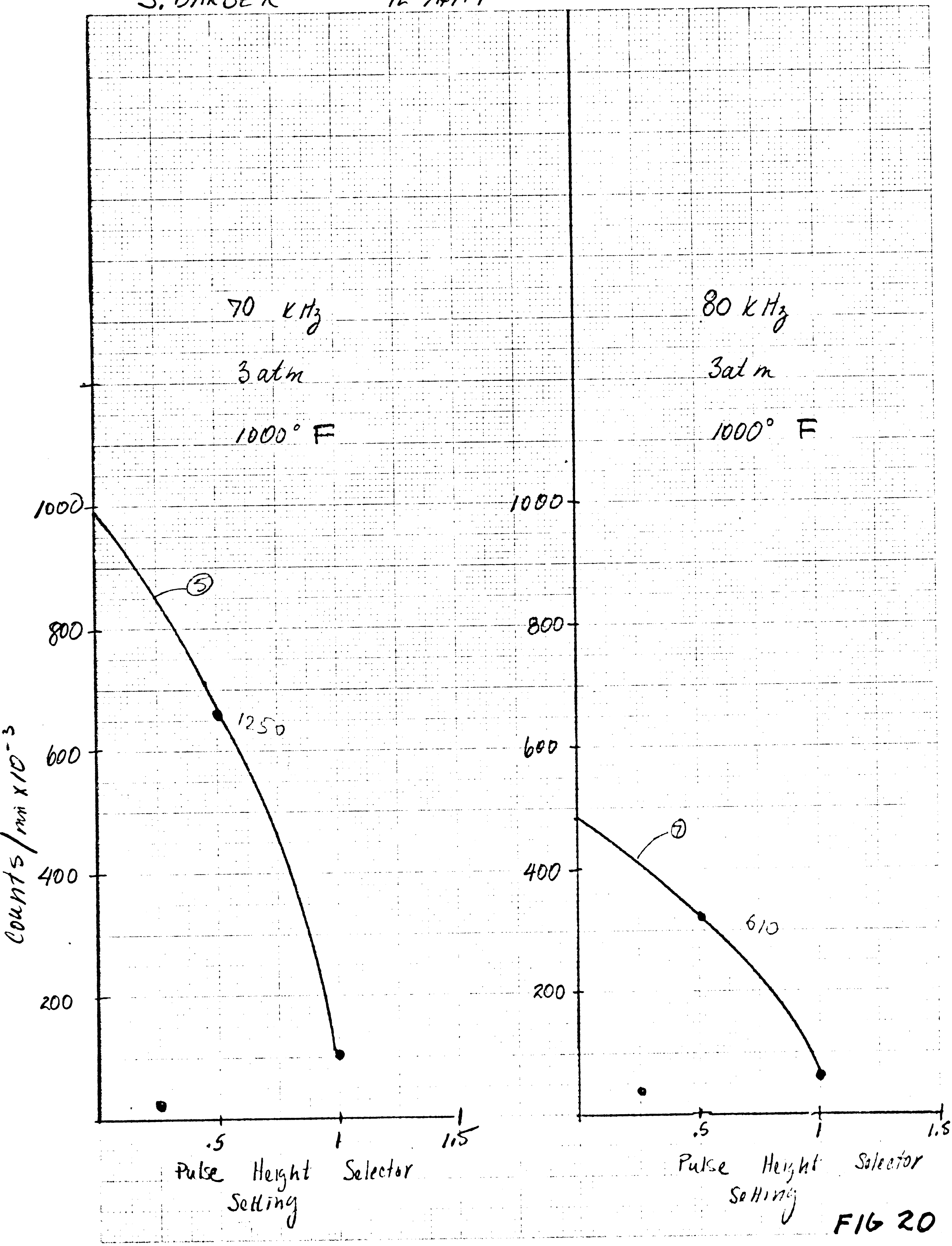

FIG 20

S. BARBER 12 April 1976

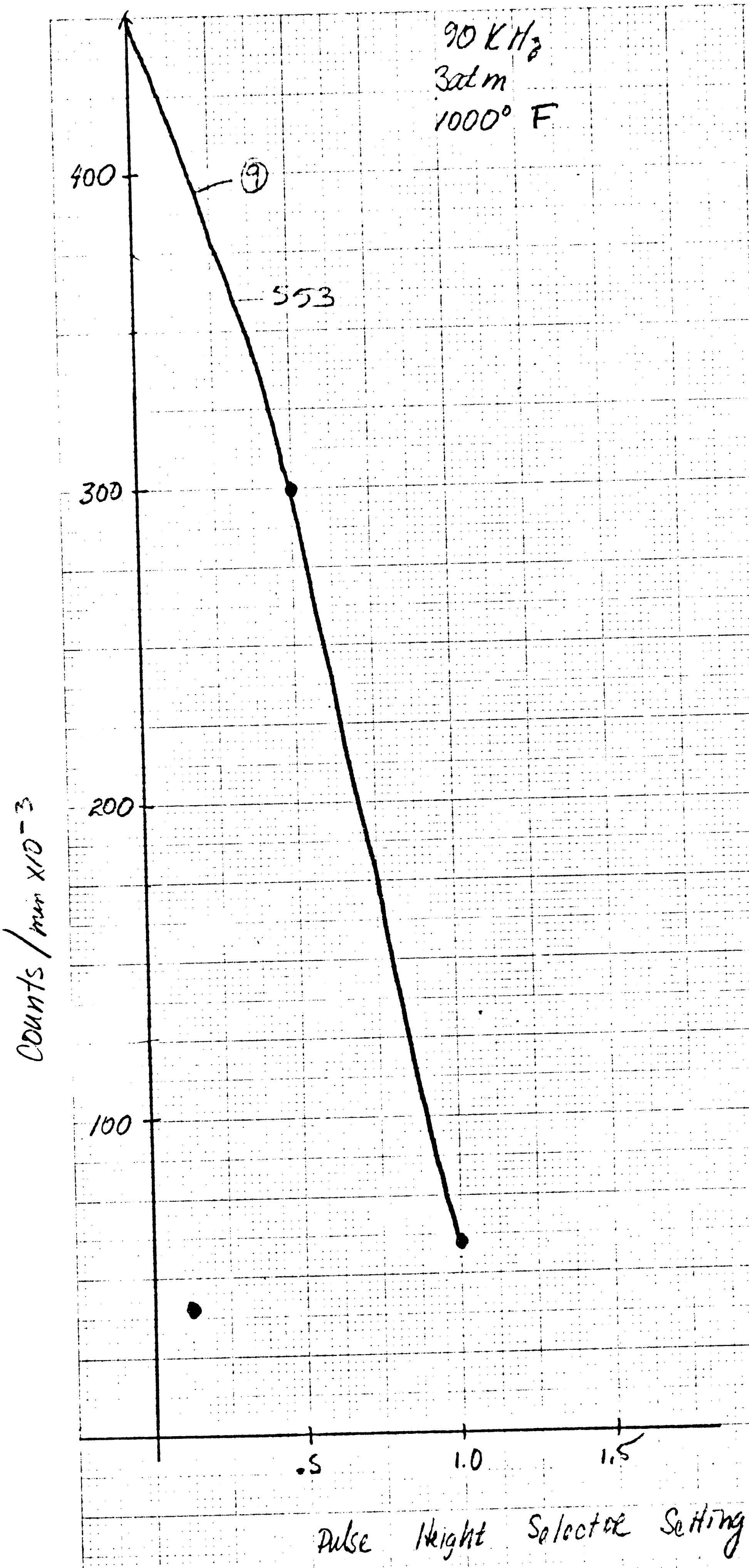

FIG 21

0 Squares to the Inch

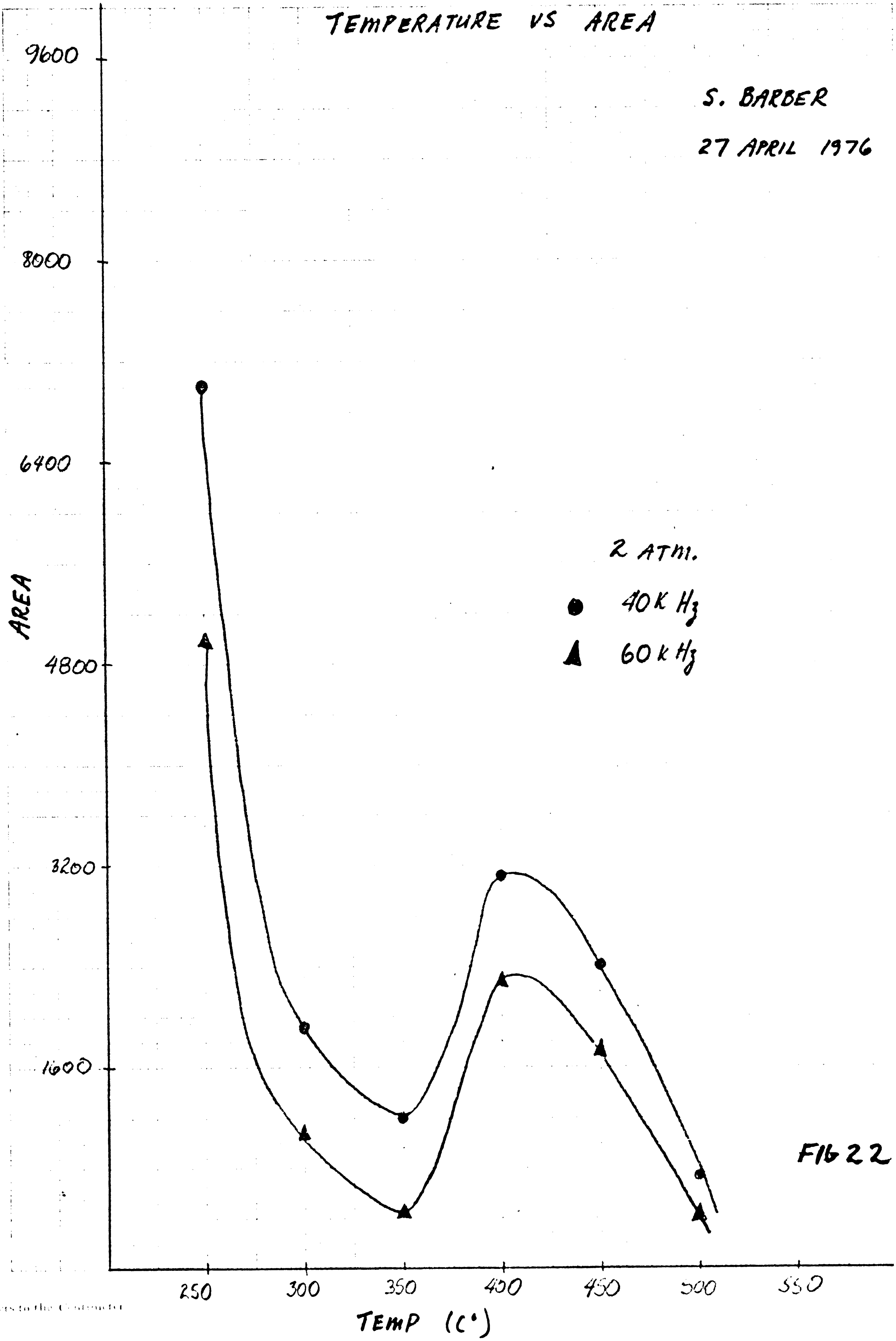
TEMPERATURE VS AREA
S. BARBER
27 APRIL 1976
9600
8000
6400
4800
3200
1600
AREA
2 ATM.
40 K Hz
60 K Hz
250
300
350
400
450
500
550
TEMP (C°)

FIG 22

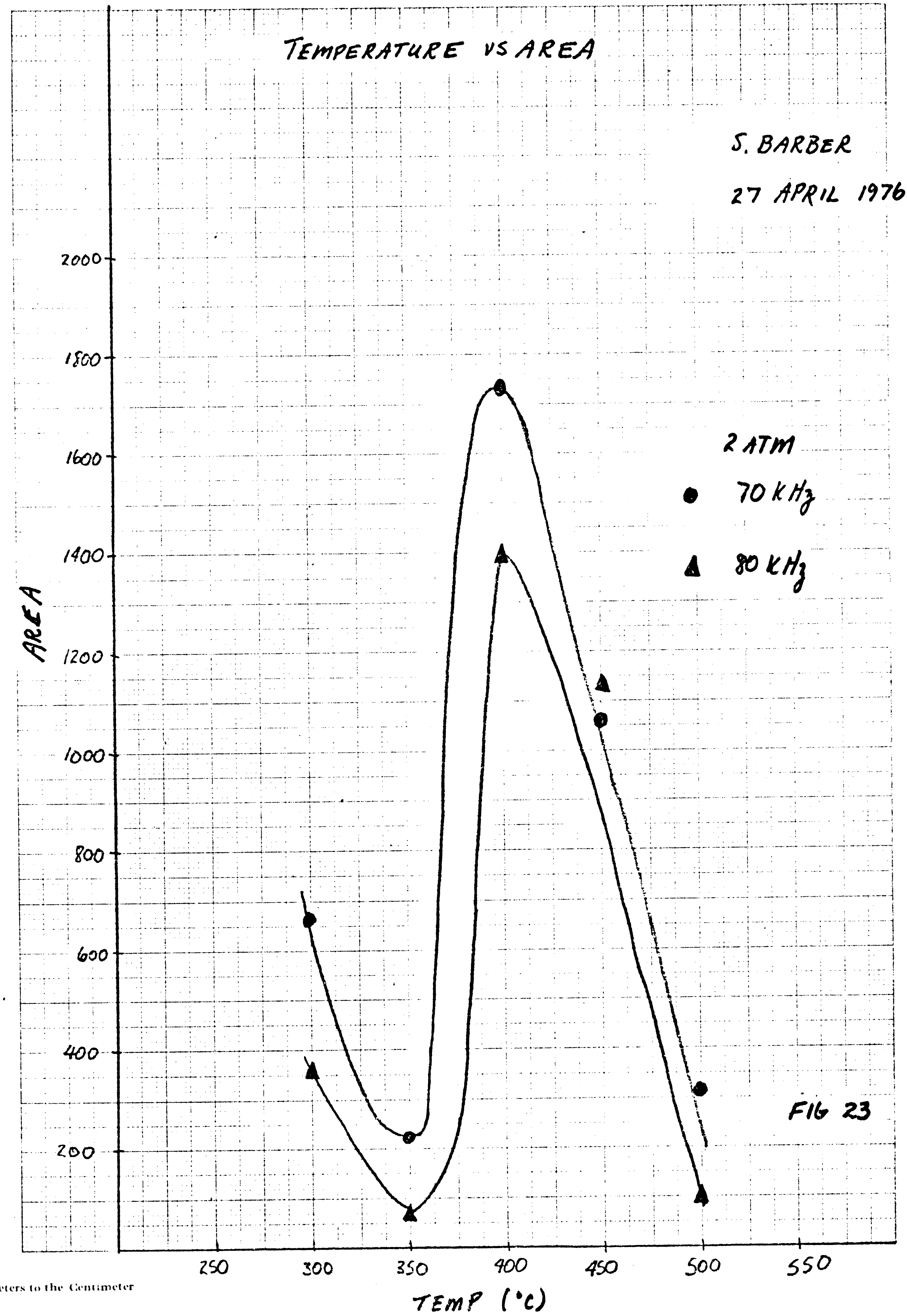
TEMPERATURE VS AREA
S. BARBER
27 APRIL 1976
2 ATM
70 kHz
80 kHz
AREA
2000
1800
1600
1400
1200
1000
800
600
400
200
250
300
350
400
450
500
550
TEMP (°C)
FIG 23

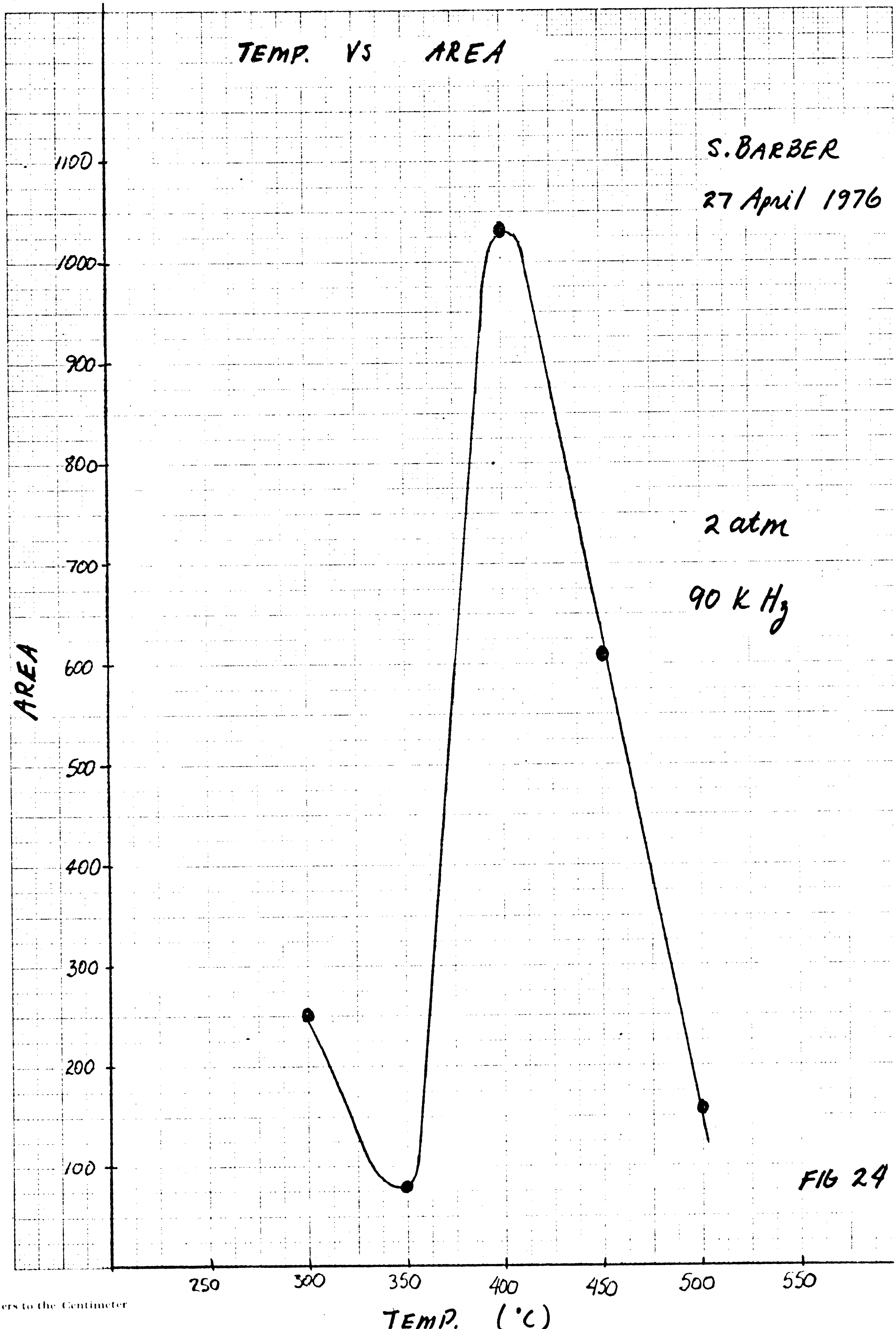
TEMP. VS AREA
S. BARBER
27 April 1976
2 atm
90 K Hz
AREA
1100
1000
900
800
700
600
500
400
300
200
100
250
300
350
400
450
500
550
TEMP. (°C)

FIG 24

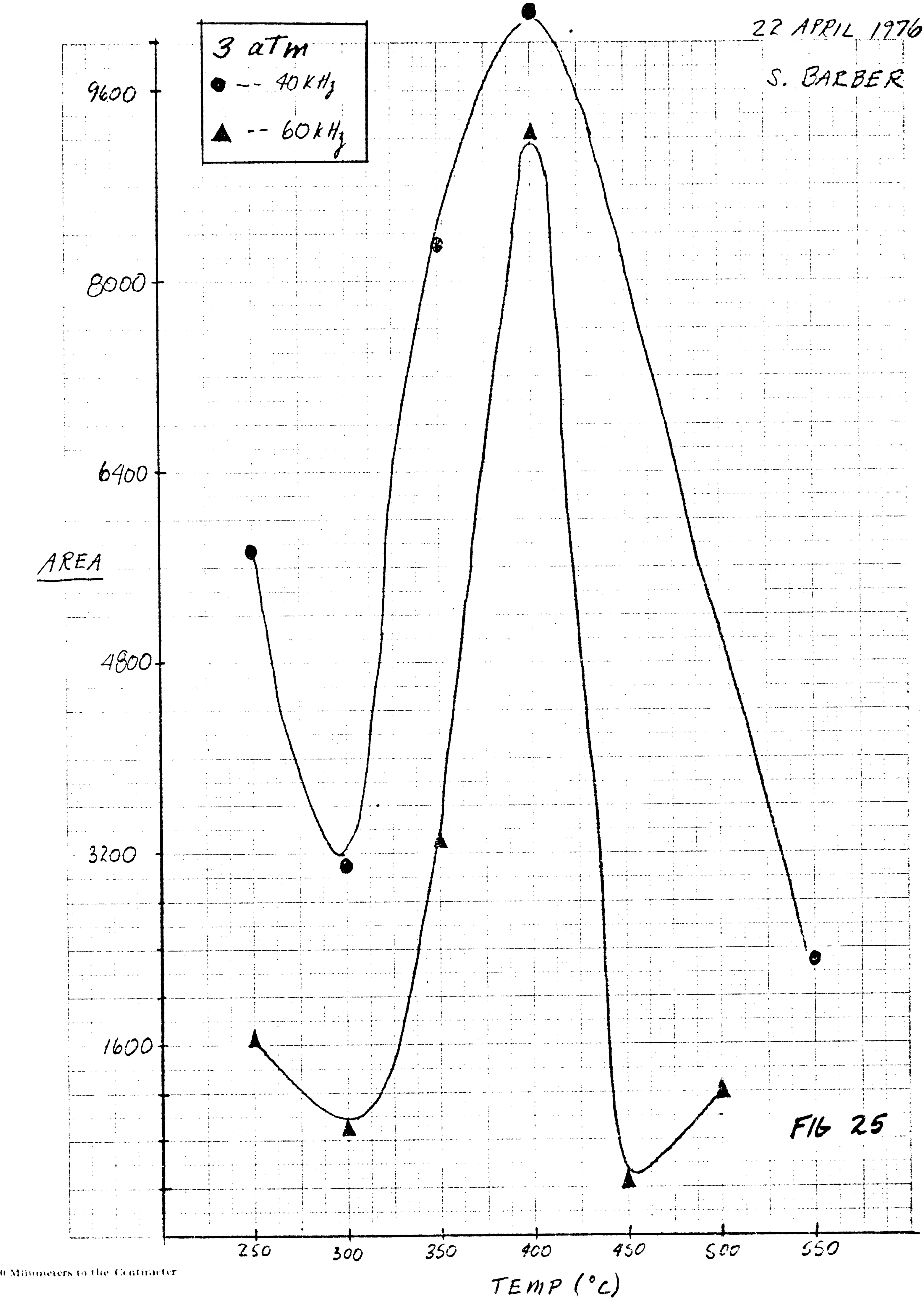

22 APRIL 1976
S. BARBER
3 atm
● -- 40 kHz
▲ -- 60 kHz
9600
8000
6400
AREA
4800
3200
1600
250
300
350
400
450
500
550
TEMP (°C)
0 Millimeters to the Centimeter

FIG 25

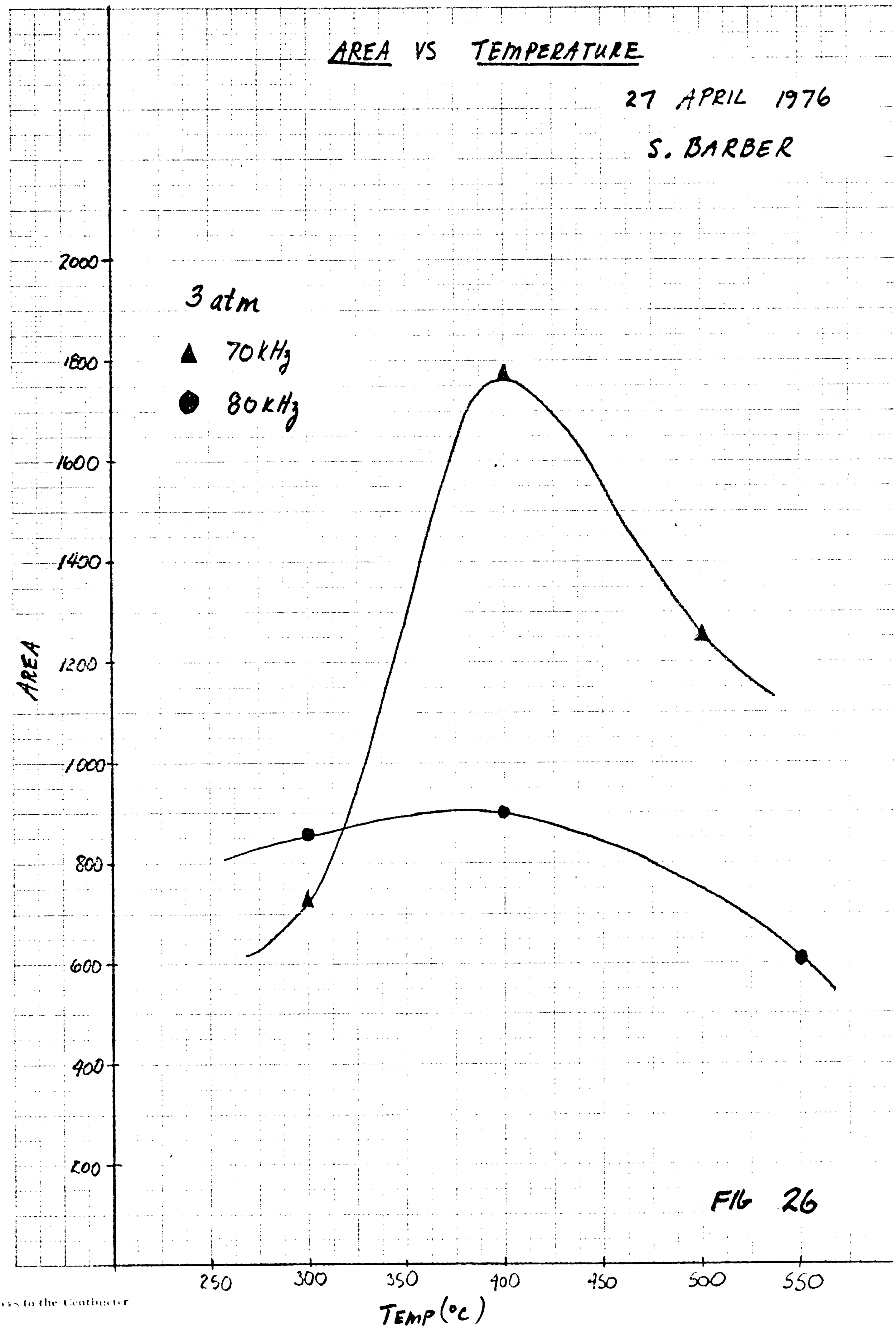

AREA VS TEMPERATURE
27 APRIL 1976
S. BARBER
3 atm
70 kHz
80 kHz
AREA
2000
1800
1600
1400
1200
1000
800
600
400
200
250
300
350
400
450
500
550
TEMP (°C)

FIG 26

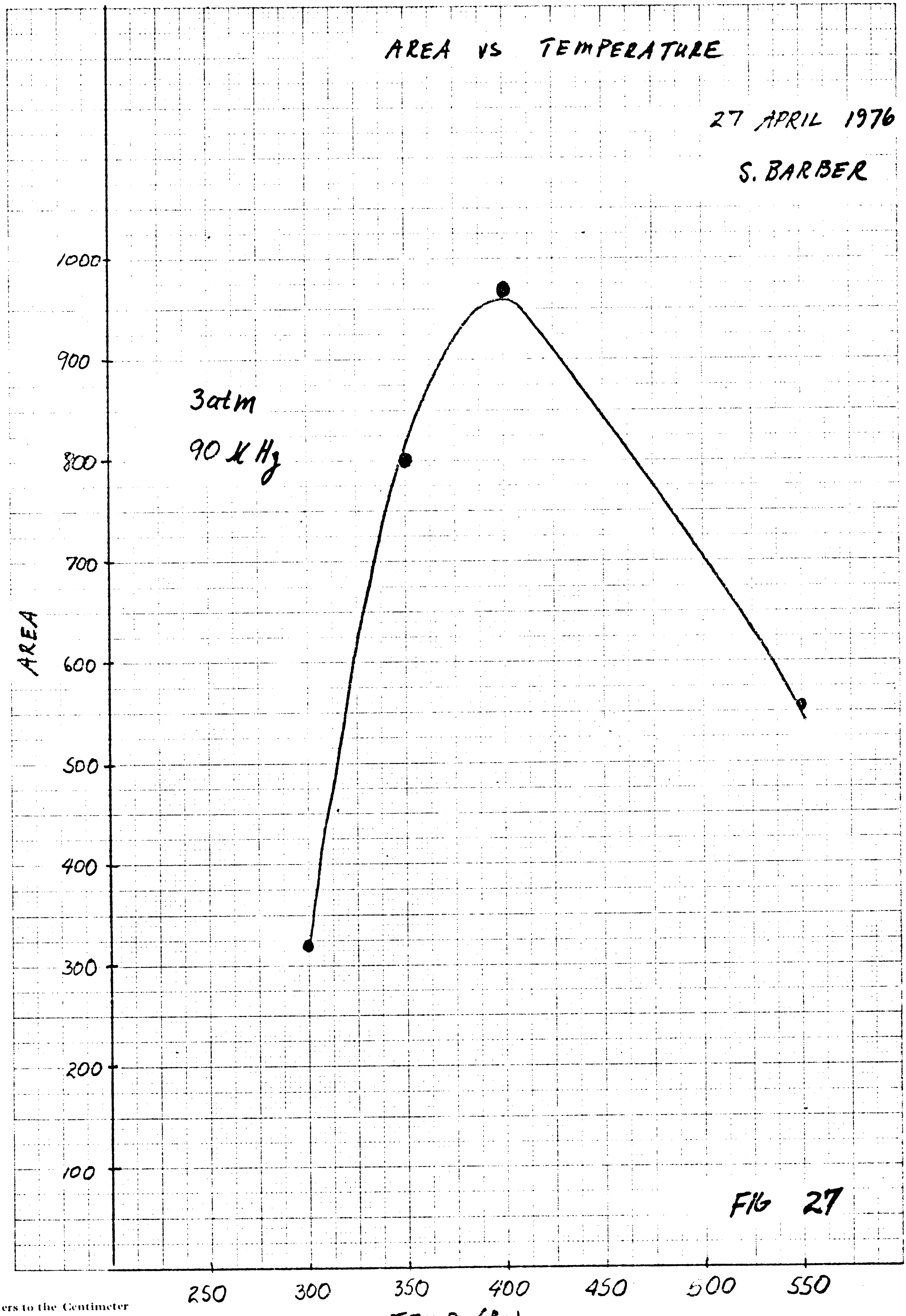
AREA VS TEMPERATURE
27 APRIL 1976
S. BARBER
1000
900
800
700
600
500
400
300
200
100
AREA
3atm
90 kHz
250
300
350
400
450
500
550
TEMP (°c)

FIG 27

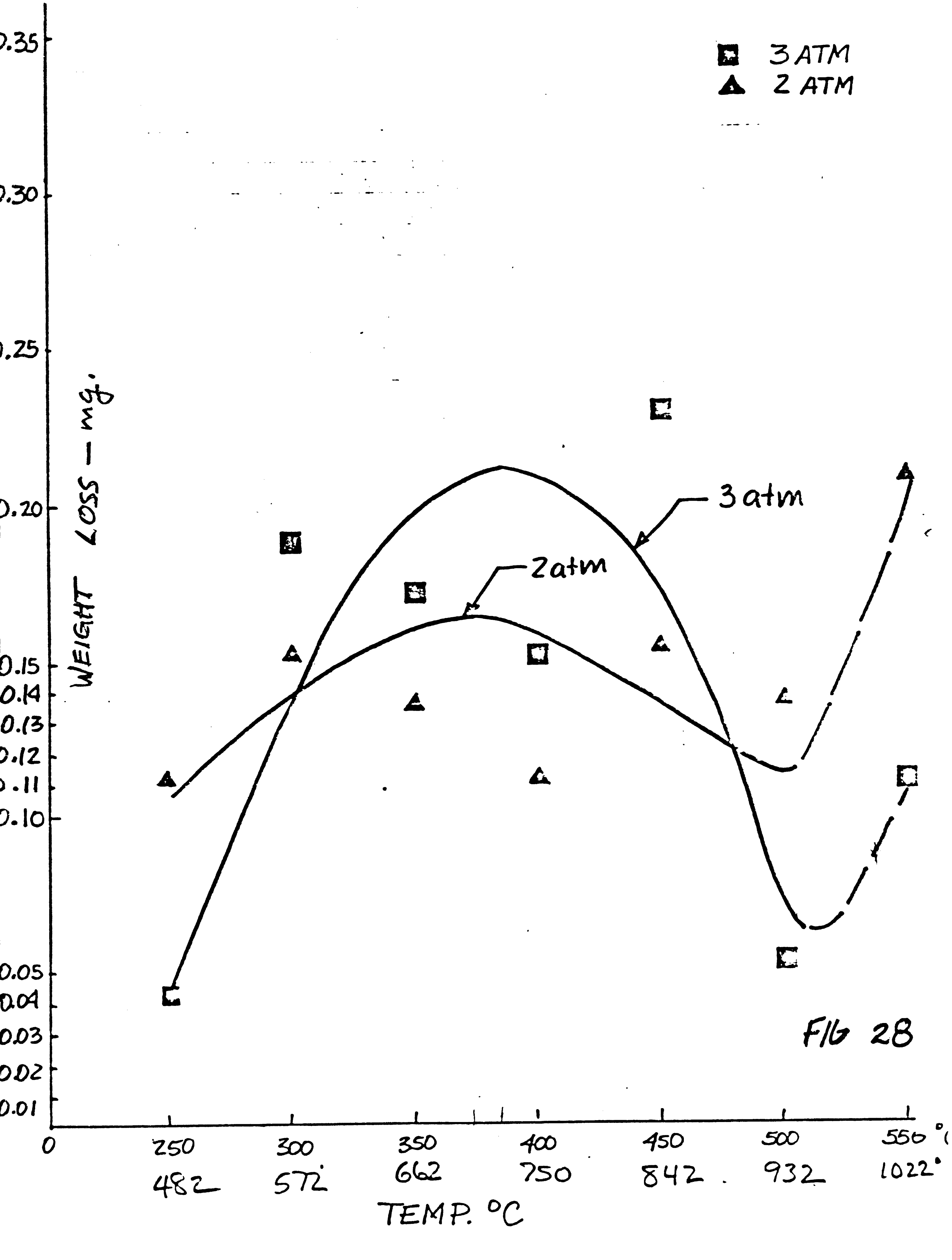
3 ATM
2 ATM
3atm
2atm
WEIGHT LOSS - mg.
.35
.30
.25
.20
0.15
0.14
0.13
.12
.11
0.10
0.05
0.04
0.03
0.02
0.01
0
250
482
300
572
350
662
400
750
450
842
500
932
550
1022
TEMP. °C

FIG 2B

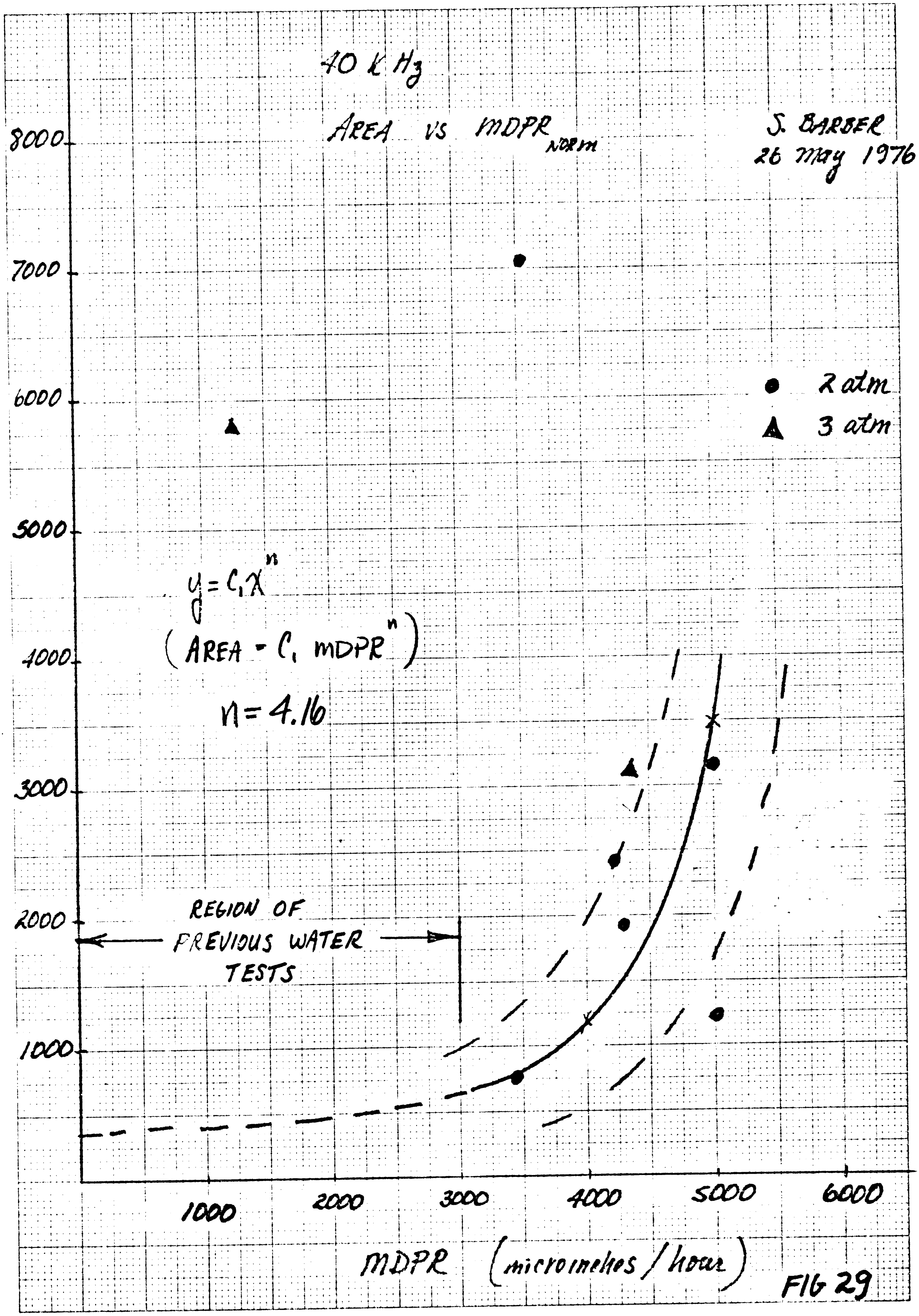
40 kHz
AREA VS MDPR NORM
S. BARBER
26 May 1976
8000
7000
6000
5000
4000
3000
2000
1000
2 atm
3 atm
y = C1 X^n
(AREA = C1 MDPR^n)
n = 4.16
REGION OF PREVIOUS WATER TESTS
1000
2000
3000
4000
5000
6000
MDPR (micromhos / hour)

FIG 29

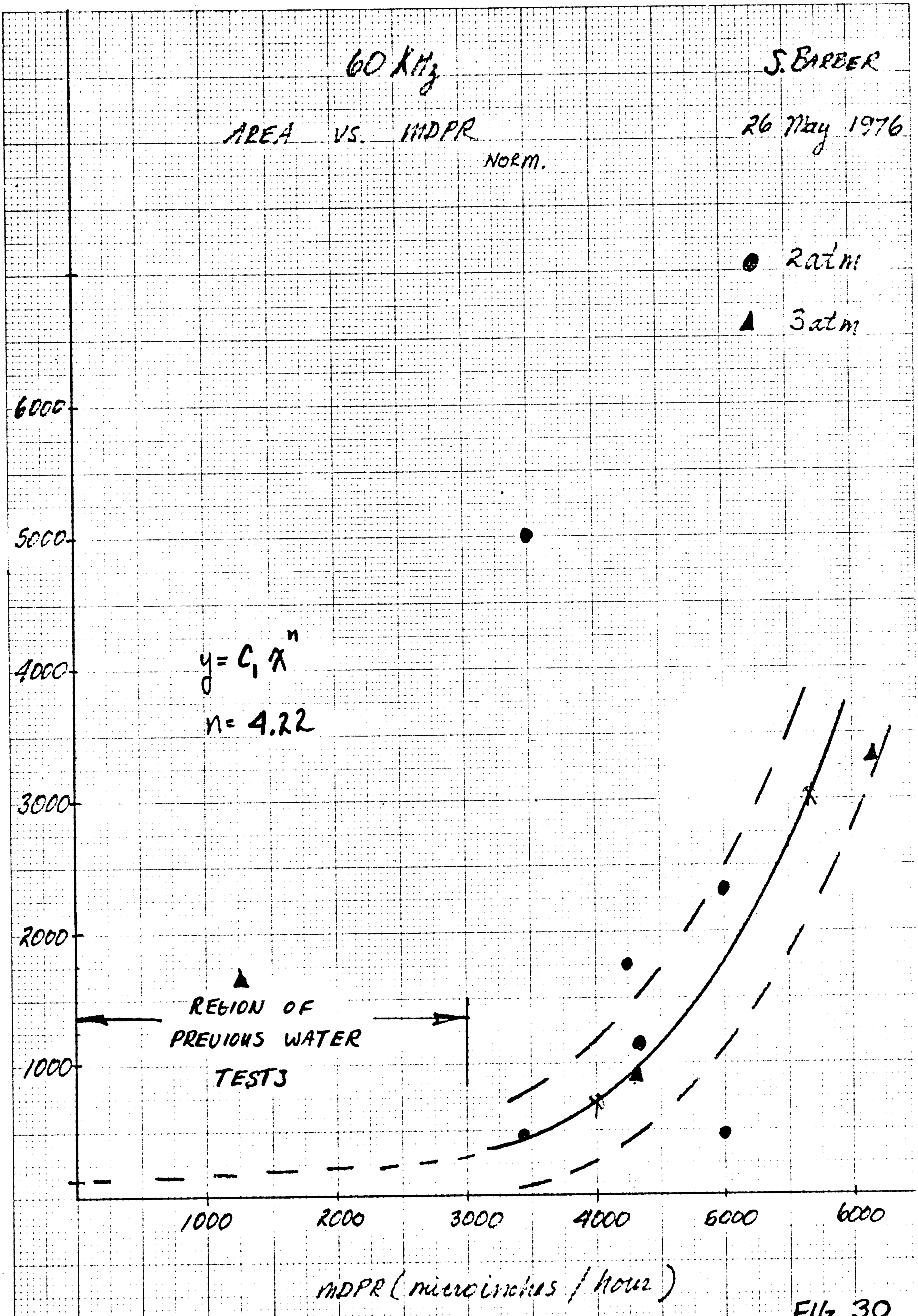
60 KHz
S. BARBER
AREA VS. MDPR NORM.
26 May 1976
2atm
3atm
$y = C_1 x^n$
n = 4.22
REGION OF PREVIOUS WATER TESTS
6000
5000
4000
3000
2000
1000
1000
2000
3000
4000
6000
6000
MDPR (microinches / hour)

FIG 30

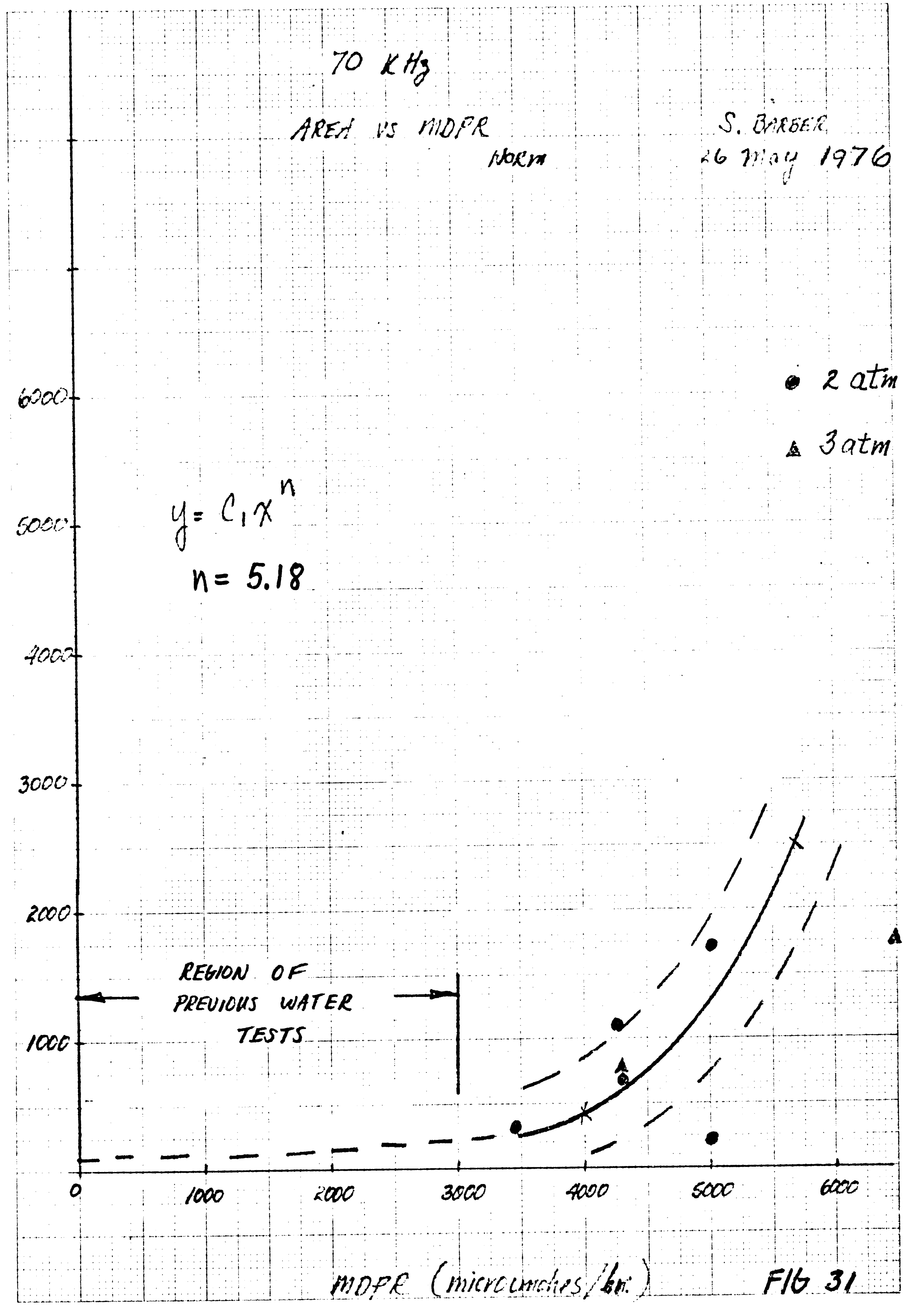

FIG 31

0 Squares to the Inch

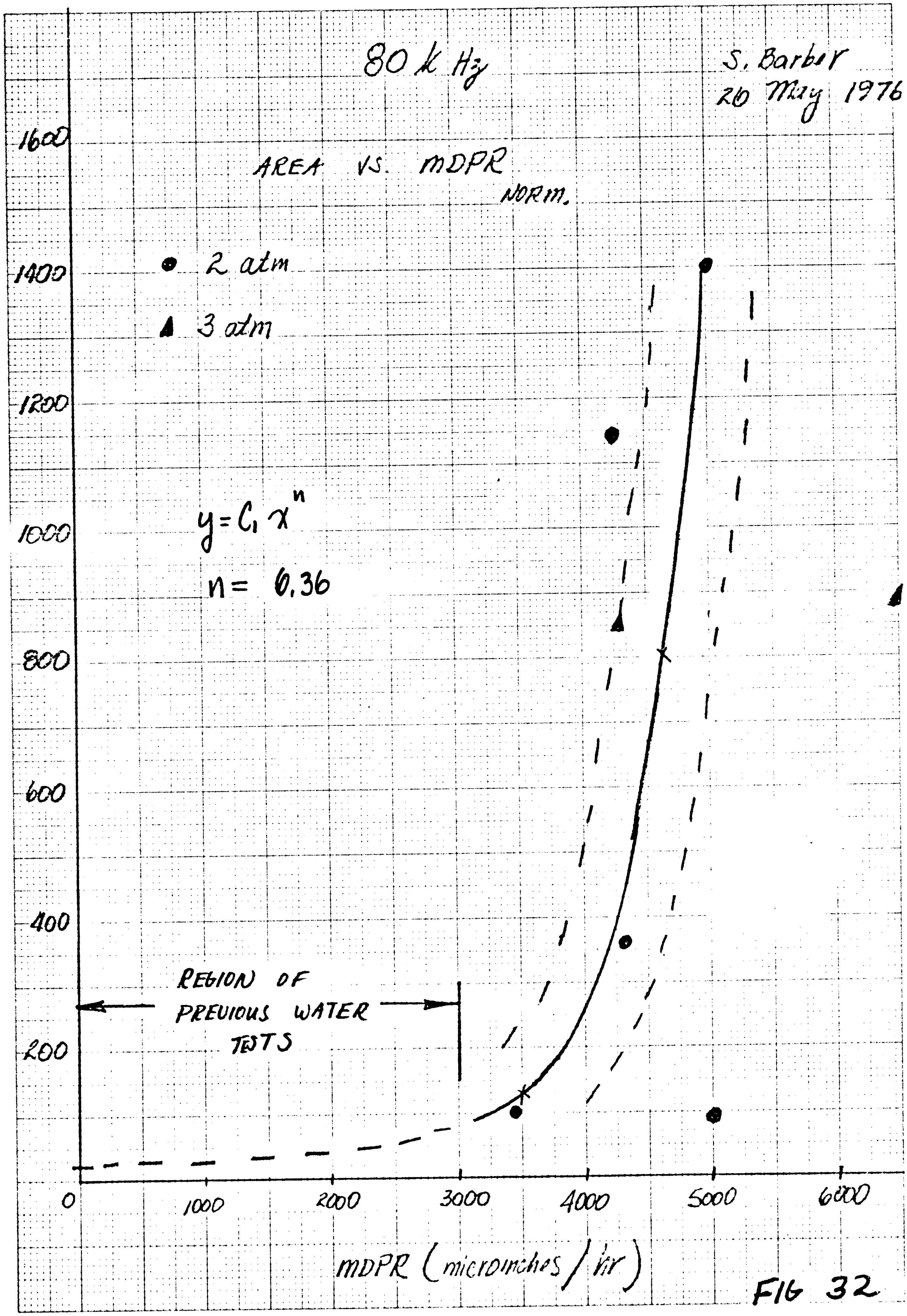

80 k Hz
S. Barber
20 May 1976
AREA VS. MDPR
NORM.
2 atm
3 atm
$y = C_1 x^n$
$n = 0.36$
REGION OF PREVIOUS WATER TESTS
1600
1400
1200
1000
800
600
400
200
0
1000
2000
3000
4000
5000
6000
MDPR (microinches / hr)

FIG 32

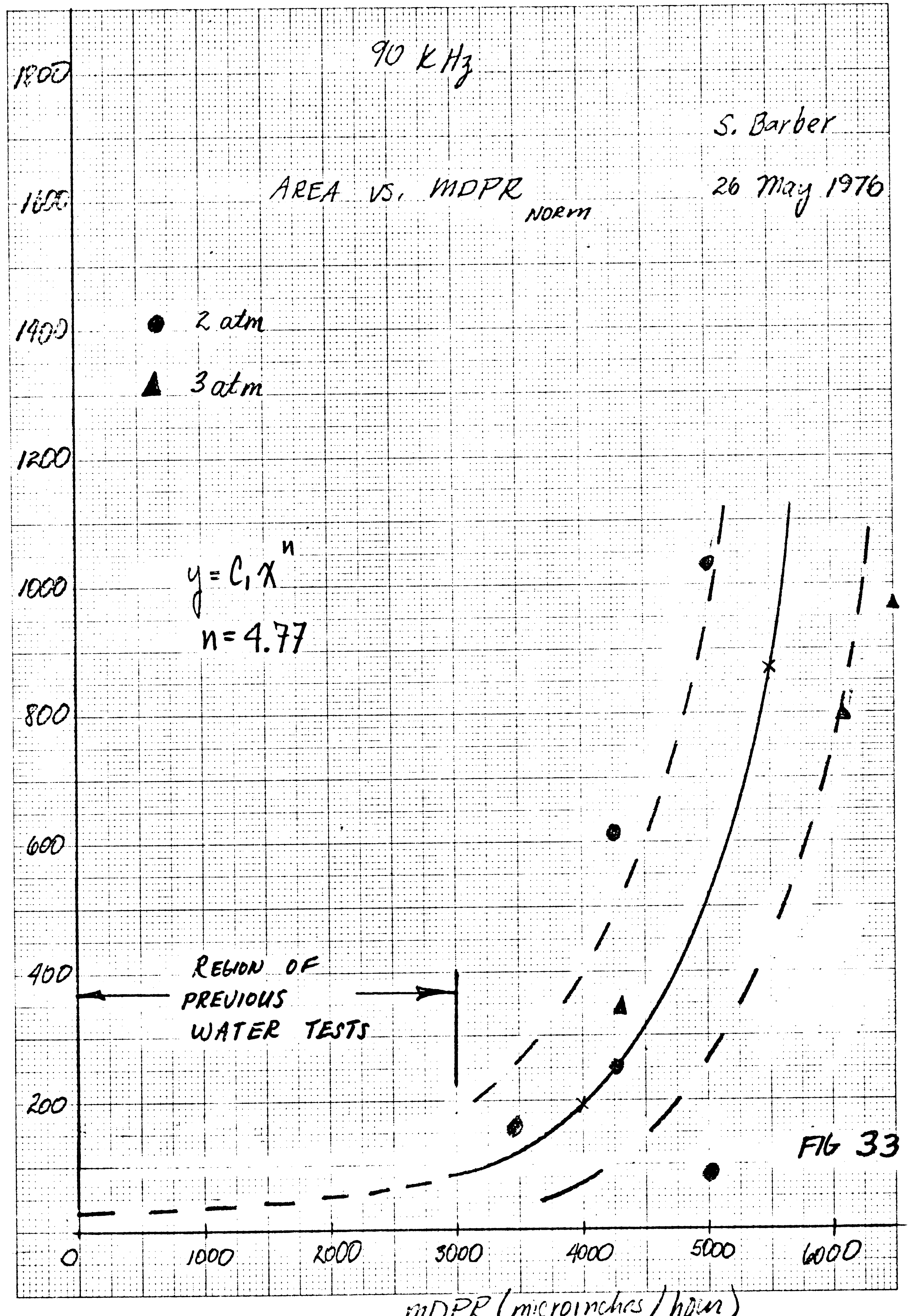

FIG 33

10 Squares to the Inch

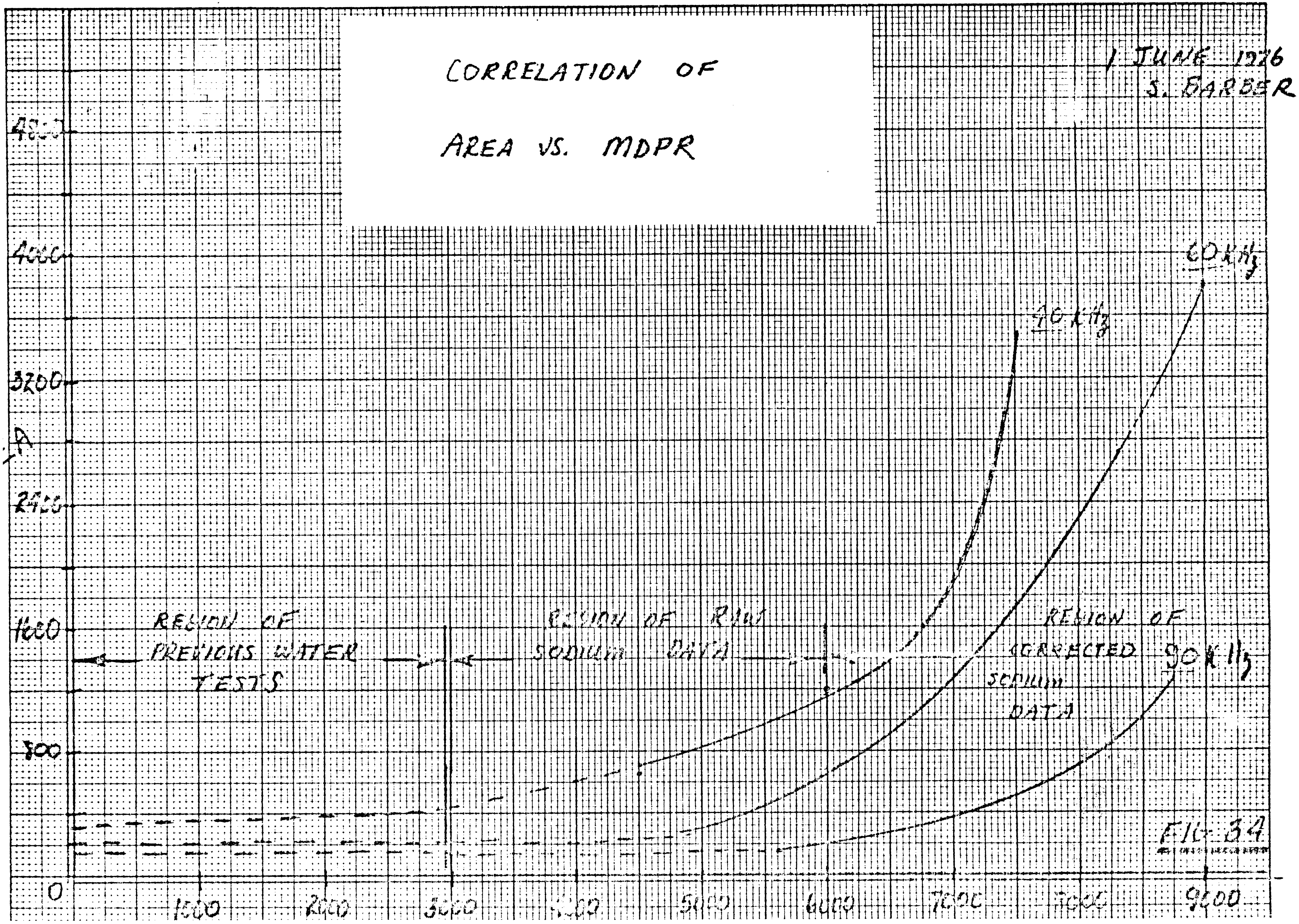
CORRELATION OF
AREA VS. MDPR
1 JUNE 1976
S. BARBER
60 KHz
40 KHz
90 KHz
A
4000
3200
1600
800
0
REGION OF PREVIOUS WATER TESTS
REGION OF RAW SODIUM DATA
REGION OF CORRECTED SODIUM DATA
1000
2000
3000
5000
6000
7000
9000
FIG. 34